Websites:
http://www.lifesciencesite.com
http://www.sciencepub.net

Emails:
editor@sciencepub.net
sciencepub@gmail.com

Life Science Journal

MARSLAND PRESS
Multidisciplinary Academic Journal Publisher

Different Mutations in the NADPH Oxidase Enzyme lead to Different Macrophage Responses

Suhailah Khalil Abdulhalim, Dr.Dean Willis

University College London, Gower Street
UK, London WC1E 6BT, Tel: +44 (0) 020 7679 2000
*Correspondence: suhailahak@hotmail.com

Abstract: Chronic granulomatous disease (CGD) is a genetic disease characterised by a dysfunctional NADPH oxidase with a reduced capacity to produce the reactive oxygen species (ROS) needed to defend against pathogens. Mutations in the various subunits of the NADPH enzyme may lead to the manifestation of CGD. In this study, we theorise that different mutations in the subunits of NADPH oxidase result in an altered macrophage response to infection. LPS was found to decrease macrophage viability but also cause increased production of TNFa and IL-1b. The build up of dead macrophages may also contribute to the inflammatory response, characterised by TNFα and IL-1β release from the remaining active cells. PMA; used to differentiate U937 cells into macrophages, becomes cytotoxic to macrophages in a time and dose-dependent fashion. Our hypothesis that mutations in the subunits of NADPH oxidase affect the macrophage response to TLR and inflammasome response was confirmed. However, repeat experimentation and further investigations are necessary to further our understanding of the pathogenesis of CGD.
[Suhailah Khalil Abdulhalim, Dr.Dean Willis. **Different Mutations in the NADPH Oxidase Enzyme lead to Different Macrophage Responses**. Life Sci J 2023;20(2):29-64]. ISSN 1097-8135 (print); ISSN 2372-613X (online). http://www.lifesciencesite.com.04.doi:10.7537/marslsj200223.04.

Key Words: CGD, X-linked disorders, NADPH oxidase enzyme and Mutations in genes.

List of Abbreviations

Abbreviation	Definition
AP-1	Activator Protein-1
AU	Absorbance Unit
BSA	Bovine serum albumin
CGD	Chronic granulomatous disease
Con	Control
CYBA	cytochrome b-245 alpha ($p22^{phox}$)
CYBB	cytochrome b-245 beta ($gp91^{phox}$)
DMSO	Dimethyl sulfoxide
ELISA	Enzyme-Linked Immunosorbent Assay
FCS	Foetal calf serum
gp	glycoprotein
H_2O_2	hydrogen peroxide
HRP	Horseradish peroxidase
IL-1β	Interleukin-1β
LPS	Lipopolysaccharide
Ml	Millilitre ($10\ L^{-3}$)
MSU	Monosodium urate
MTT	3-(4;5-dimethylthiazol-2-yl)-2;5-diphenyltetrazolium bromide
NADPH	nicotinamide adenine dinucleotide phosphate
NF-κB	Nuclear factor kappa enhancer of activated B cells
NOX	NADPH oxidase
OD	Optical density
PBRsiRNA	Poly Basic Region siRNA
PBS	Phosphate buffered saline
Phox	phagocytic oxidase
PMA	Phorbol-12-myristate-13-acetate
PML	polymorphonuclear leukocytes

RNAi	RNA Interference
ROS	Reactive oxygen species
siRNA	Small Interfering RNA
Sp. / spp.	Species
TLR	Toll-like receptor
TMB	3;3';5;5'-Tetramethylbenzidine chromogenic substrate
TNF (α)	Tumour necrosis factor (alpha)

Chapter 1

1.0 Introduction

The host immune system employs a plethora of defence mechanisms to protect against infection by pathogenic microorganisms. The result is a multifaceted defence mechanism, employing a myriad of immune cells, signalling proteins and small molecules that forms an intrinsic part of both the innate and adaptive immune systems. The following literature review aims to provide background information on these host defences, with a focus on phagocytosis by macrophages and the subsequent oxidative burst, mediated by respiration by NADPH oxidase enzyme. This review will outline the physiological and biochemical mechanisms underpinning this critical defence mechanism and will concentrate on one well-characterised condition arising from mutations in the NADPH oxidase system: chronic granulomatous disease. The decreased (or absent) of the oxidative burst in leukocytes seen in CGD is due to one or more inherited mutations in genes encoding subunits of the enzyme complex. This review will detail the impact of these mutations on NADPH oxidase formation and activity and highlight existing therapeutic intervention strategies to treat CGD.

Literature Review

1.1 Genetic diseases

Genetic diseases can result from either a single mutated gene (single gene disorder) or they can be 'polygenic', involving biological systems linked to environmental factors. It has been reported that there are more than 4,000 human diseases caused by single gene defects, many of which are heritable (Kumar, 2008). One type of heritable genetic disorder is 'autosomal inheritance', in which genetic traits located on the one of the twenty-two non-sex determining chromosomes (autosomes). Autosomal inheritance can be either dominant or recessive, referring to whether or not traits are expressed when two alleles are present. Recessive traits are only expressed phenotypically when two copies of the same allele are inherited (homozygous). In cases where both parents are carriers of an autosomal recessive trait the offspring have a 25% chance of the disease being inherited and a 50% chance of the offspring becoming carrier for the disease. The probability of an offspring inheriting an autosomal recessive trait is less than when the condition is autosomal dominant, where only one mutated copy of a gene is required to express the allele.

Another form single gene disorder is X-linked inheritance, where the mutated gene causing the disorder is located on the X-chromosome. Because females have two X-chromosomes, disorders on this chromosome are less likely to manifest, compared to males. However, females with one copy of a mutated gene on an X-chromosome can become carriers of the genetic condition. In contrast, males with only one copy of the X-chromosome are susceptible to the effects of mutated genes that cause an estimated 651 X-linked disorders (OMIM Statistics, 2013).

In addition to single gene disorders, there are a growing number of multifactorial disorders (e.g. heart disease, diabetes and cancer), which may have a genetic element, but the incidence rate also depends on environmental factors and there is no definitive pattern of inheritance. Furthermore, complex disorders are more difficult to diagnose and treat due to the lack of knowledge of the causes and the impact of contributing factors.

This dissertation will focus on mechanisms underpinning the single gene disorder chronic granulomatous disease (CGD), According to Kang *et al.* (2011) the majority of cases of CGD are X-linked; the condition is referred to as an 'X-linked trait', although, as will be discussed, the condition can also be transmitted in an autosomal recessive manner. Epidemiological data from van den Berg *et al*. (2009) is representative of CGD studies, finding that 67% of CGD cases were X-linked i.e a mutation in the $gp91^{phox}$ subunit. In accordance with heritability traits for other X-linked disorders, the authors reported that 98% of patients with X-linked CGD were males (n=290).

1.2 Chronic Granulomatous Disease (CGD).

CGD is a heritable disorder characterised by a deficiency of host immune cells to produce reactive oxygen species (ROS), which form an important part of the defence against pathogens (Pizzolla *et al.*, 2012). Production of the superoxide radical (O_2^-) by NADPH oxidase represents a particularly important component of this defence mechanism (Cross *et al.*, 1994; Krause, 2007), and mutations in the NADPH oxidase typically lead to symptoms associated with CGD. The immune

response originates from neutrophils, monocytes, and macrophages, collectively referred to as phagocytes. In order to produce the antimicrobial oxidative burst, phagocytes require full activity of enzyme, referred to as phagocytic NADPH oxidases (Phox). Defects in this enzyme results in a weakened response against pathogens, and may lead to CGD. There are more than 410 known defects in the subunits of the Phox enzyme complex that can result in CGD (Heyworth *et al.*, 2003). CGD symptoms include bacterial infection, most frequently pneumonia, skin infections, pulmonary lymphadenopathies, osteomyelitis or abdominal abscesses (Khalilzadeh *et al.*, 2006). Because of the respiratory defect in phagocytes, sufferers of CGD are particularly susceptible to bacteria that possess catalase enzymes, which break down hydrogen peroxide, produced by host cells. The reason for this is that H2O2 is produced by superoxide and protons. Therefore the bacteria have protective mechanism against the limited amount of H2O2 produced. Catalase-producing pathogens include *Staphylococcus* spp. (Pizzolla *et al.*, 2012), *Listeria monocytogenes* (Mosser and Edwards, 2008), and *Escherichia coli* (De Ravin *et al.*, 2008) bacteria, as well as species of *Aspergillus* (Grimm *et al*., 2011) and *Candida* fungi (Kumar, 2008). The study by Pizzolla *et al*. (2012) demonstrated that the $gp91^{phox}$ component was able to demonstrate protection against lethal concentrations of the CGD-related pathogens, *Staphylococcus* spp. and *Burkholderia cepacia*, by clearing the bacteria from inside and outside of the phagosome.

According to the available scientific literature, CGD-related pathogens are usually isolated from the lungs via biopsy or bronchial lavage and the type of pathogen tends to vary between studies. However, there is some degree of inter-study consistency for some pathogens, such as the fungi *Aspergillus* spp., which is represents a 'marker' strain for cases of CGD. In North America, the five microbial pathogens most associated with CGD are *Staphylococcus aureus*, *Serratia marcescens*, *Burkholderia cepacia*, *Nocardia* spp. and *Aspergillus* spp. (Kang *et al*., 2011). In Europe, *Aspergillus* infections made up the vast majority of clinical isolates from patients with CGD and infection with *Burkholderia cepacia* was relatively rare patients (van den Berg *et al*., 2009).

In addition to infection, X-linked CGD often manifests as a granulomatous inflammation, caused by macrophages and large, multinucleated immune cells causing obstruction in multiple tissue types. When these granulomas are investigated, the majority show no evidence of pathogen involvement, and the hyper-activated immune response responds well to steroid treatment (Kang *et al*., 2011).

1.3 CGD epidemiology, diagnosis and treatment

In the United States, CGD is estimated to have an incidence rate of 1 in 200,000 people, with approximately twenty new cases identified each year (Pao *et al.*, 2004). Most large studies have shown an infection rate in CGD patients of around 0.15 to 0.3 cases per year (Kang *et al.*, 2011)

In Europe there is lower rate of CGD occurance: 1 in 250,000 people, based on a study of 429 patients (van den Berg *et al.*, 2009). The majority of cases of CGD in Europe were X-linked (67%) rather than due to an autosomal recessive allele (33%), although it is interesting to note that participants from Eastern Europe, or immigrants of Arabic, North African or Asian origin were more likely to exhibit an autosomal recessive CGD type.

A rapid high resolution genetic analysis of X-linked CGD performed by Hill *et al*. (2010) identified nineteen different mutations, which cause the disease. These mutations varied in the type (missense, nonsense and splicing) and location (exons and introns in the X chromosome), and all resulting in decreased or absent levels of oxidase activity (Hill *et al.*, 2010). Interestingly, ten of the identified mutations were previously unknown, providing a greater insight into the breadth of genetic abnormalities underpinning CGD.

CGD is diagnosed early in childhood, usually between three (Roos *et al.*, 2010) and five years of age (Winkelstein *et al.*, 2000). However, there is some inter- and intra-study variability in age of onset of CGD. For example, was confirmed in one analysis of thirteen patients in Iran, in which the mean age of onset of symptoms was 2 years, ranging from 1 month-12 years (Khalilzadeh *et al*., 2006). A multi-study review of CGD, produced by Kang *et al*. (2011), identified a median diagnosis age of 5.4 years. The early diagnosis of CGD is important to combat existing infections and prevent further microbial pathogenesis. Despite the early detection rate and the presence of a range of treatments, (Roos *et al.*, 2010) reported with a mortality rate of around 21%.

1.4 Diagnosis

A diagnosis of CGD is made commonly using the nitroblue-tetrazolium (NBT) test (Uzel *et al.*, 2010). The NBT confirms the presence of reactive oxygen species, by oxidising nitroblue-tetrazolium and eliciting a colour change (blue) in a concentration-dependent manner. Therefore, the NBT tests for the absence of reactive oxidative species, usually produced by the host PHOX enzymes. Once the diagnosis of CGD has been made, a genetic analysis may be used to determine which mutation is the cause of the condition.

Another commonly used method of diagnosing CGD is the neutrophil respiratory burst assay, coupled with flow cytometry. Briefly, the method involves incubation of

wild-type cells with the non-fluorescent compound dihydrorhodamine-1,2,3, a compound that detects the production of the superoxide anion. Once activated, the wild-type neutrophils produce the fluorescent, oxidised metabolite, rhodamine-1,2,3, which can be detected by flow cytometry. In X-linked CGD, phagocytic cells do not produce the mutated NADPH oxidase, and dihydrorhodamine-1,2,3 oxidation does not occur (Hill *et al*., 2010). In addition to the classic X-linked CGD, in which there is no NADPH oxidase activity, rarer 'variant' X-linked forms of CGD exist in which there is some residual ROS production from the mutated NADPH oxidase (Bu-Ghanim *et al.*, 1995). Variant X-linked CGD may involve normal concentrations of NADPH oxidase subunits expressed by immune cells however the oxidase activity is absent. Alternatively the mutation may lead to decreased expression of the enzyme in addition to reduced activity. Both of these forms of variant X-linked CGD can be detected through the neutrophil respiratory burst assay. However, one important limitation of the flow cytometry approach is the inability to distinguish between autosomal recessive and X-linked forms of CGD. Other technical challenges of this diagnostic method remain, including the requirement of activating neutrophils for the assay, depletion of the cellular respiratory activity over time and the possibility of pre-activation of neutrophils by infection or contamination; all of which will lead to a mixed population of florescent cells, and decrease reliability of the flow cytometry analysis (Hill *et al*., 2010).

According to Hill *et al*. (2010) there are more than 500 mutations in *CYBB*, encoding gp91^{phox}. These include missense, nonsense, deletions, insertions, spliced genes, and mutations in gene promoter sites. The array of mutations can be detected by genetic analysis, including sequencing of the *CYBB* gene. Although genetic techniques are powerful enough to distinguish the type of mutation resulting in CGD, at present there are relatively few institutions able to provide a detailed genetic analysis. With the recent development of more sophisticated sequencing technologies, in future genetic analyses may become a more common method of CGD diagnosis.

As patients with CGD have a diminished immune system, management of the condition revolves around treating and preventing pathogenic infections. This is commonly achieved by administering antibiotic or antifungal treatments, to be used as a prophylaxis against future infections. For example, a case of *Aspergillus* osteomyelitis presenting in a five year old boy was treated with a mixture of the polyene antifungal drug, Amphotericin B (1 mg/kg/day) and interferon-γ (50 μg/m^2, every two days). This regime, followed for four weeks, resulted in successful treatment of invasive aspergillosis in the patient and prevented further fungal infection (Mamishi *et al.*, 2005). Although interferon-γ treatment for CGD has been well-documented, there are some associated side-effects (e.g. fever, fatigue, abdominal pain) that can arise. Marciano *et al.* (2004) reported 37% of patients in one trial exhibited an adverse effect to interferon-γ treatment, although the authors stated that none of these effects were life-threatening.

1.5 NADPH Oxidase in macrophages

As discussed, CGD is primarily an X chromosome-linked disorder, which in the majority of cases is caused by mutations in the cytochrome b-245 beta encoding (*CYBB*) gene, found at the chromosomal locus Xp21.1 (Segal *et al.*, 2000) and encoding the membrane-bound gp91^{phox} protein subunit. This protein is a fundamental component of the NADPH oxidase complex (Segal *et al*., 2012). It has been shown that patients who are gp91^{phox} deficient have largely suppressed NADPH function, and produce lower levels of ROS (Hill *et al.*, 2010), a hallmark of CGD. Although gp91^{phox} mutations account for a large proportion of CGD cases, the disorder can also result of a defective NADPH oxidase subunit otherthan gp91^{phox}.

NADPH consists of seven subunits: a Rho guanosine triphosphatase, and five glycoprotein phagocytic oxidase (Phox) units (gp91^{phox}, p22^{phox}, p40^{phox}, p47^{phox} and p67^{phox}) (Segal *et al.*, 2012). In a non-stimulated, resting state, the subunits are segregated into membrane-bound (gp91^{phox}, p22^{phox}), and cytosolic subunits (p47^{phox}, p67^{phox}, p40^{phox}), the Rho-related C3 botulinum toxin substrate (Rac) and the GTP-binding protein, Rap1. The formation of membrane-bound heterodimers (gp91^{phox} and p22^{phox}) is essential for so-called catalytic activity (enzyme activation and subsequent formation of ROS) (von Löhneysen *et al.*, 2010).

The cytoplasmic components relocate to the membrane upon NADPH activation (Figure 1). Activity of gp91^{phox} is stimulated by this protein relocation event, which includes Rac and Rap1, allowing the formation of a complete, catabolically-active NADPH oxidase. After activation, NADPH is oxidised to $NADP^+$ (NADPH + $2O_2 \leftrightarrow NADP^+ + 2O_2^- + H^+$) and the resulting electrons are transported down a reducing potential gradient that uses oxygen as a terminal electron acceptor when oxygen (O_2) is converted to the superoxide anion (O_2^-) (Figure 1). Superoxide is unstable and in cells reacts with biological macromolecules (e.g. nucleic acids, proteins, lipids) causing oxidative stress and cellular damage (Vignais, 2002). Furthermore, O_2^- can be spontaneously reduced to hydrogen peroxide (H_2O_2), which can be converted to the hydroxyl anion (OH^-) or, using halides (e.g. Cl^-), can form hypohalous acid (e.g. $HOCl^-$), all of which have a cytotoxic effect and are utilised by the immune system as part of host defence (Hazen *et al.*, 1996; Segal and Abo, 1993).

Life Science Journal

Websites:
http://www.lifesciencesite.com
http://www.sciencepub.net

Emails:
editor@sciencepub.net
sciencepub@gmail.com

MARSLAND PRESS
Multidisciplinary Academic Journal Publisher

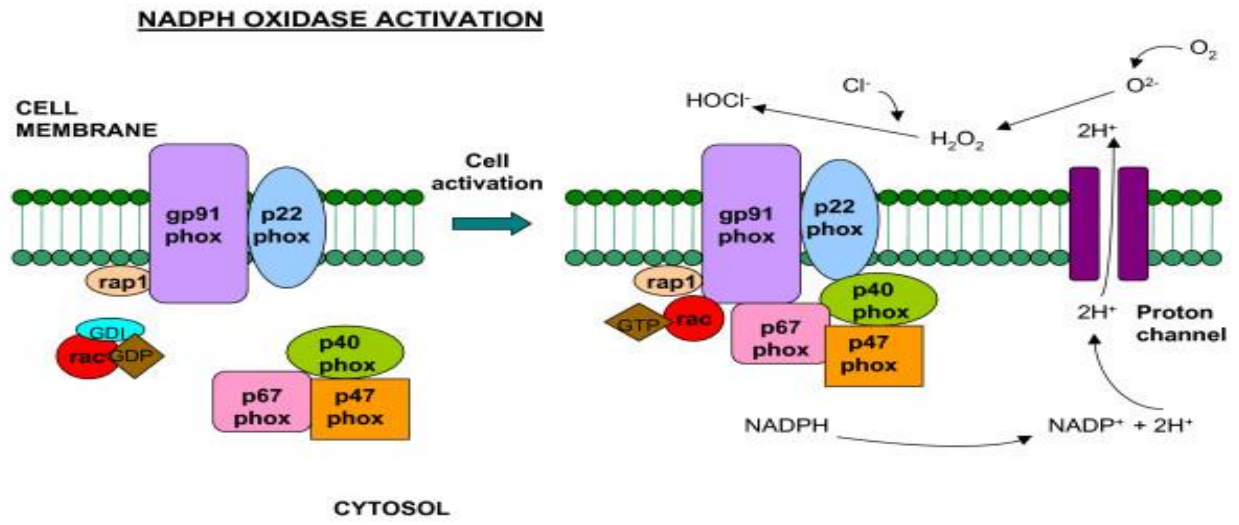

Figure 1: Schematic overview of macrophage NADPH oxidase activation. Figure from (Assari, 2006)

The NADPH subunits are structurally distinct with molecular site recognition, regulation of electron flow and catalytic activity dependent on a few conserved amino acid sequences. For example, von Löhneysen *et al*. (2010) identified the amino acids arginine (R73, R80, R91, and R92), leucine (L94) and aspartic acid (D95) in the B-loop of gp91^{phox} as being important for the catalytic activity of the enzyme. In the cell membrane, gp91^{phox} is present in complex with the smaller subunit p22^{phox}. The complex is composed of a light (alpha) chain and a heavy (beta) chain. The alpha chain (p22^{phox}) is encoded by the *CYBA* gene in humans (Hill *et al*. 2010), and mutations in the gene are associated with autosomal recessive CGD (Song *et al*., 2011). In the protein complex, gp91^{phox} forms the heavy beta chain, encoded by *CYBB*. Mutations in either *CYBA* or *CYBB* results in decreased activity of the NADPH oxidase enzyme, although neutrophils are able to engulf pathogens. Once phagocytosed, however the immune cells cannot kill the pathogen, due to a defect in the cell's respiration machinery and a failure to deliver O_2^- to the phagocytic vacuole (Kang *et al*., 2011). The gp91^{phox} protein has been proposed as a primary component of the antimicrobial oxidase system in phagocytes, and deficiency in this subunit has been linked with CGD, by several research groups (e.g. Bjorgvinsdottir *et al.*, 1996; Rajakariar *et al.*, 2009; Sadat *et al.*, 2003; Zhen *et al.*, 1993). Indeed, according to Segal *et al*. (2012), mutations in gp91^{phox}, accounts for around 65% of all CGD cases, a figure confirmed by Song *et al*. (2011). In contrast, autosomal recessive forms of CGD are caused by defects of the other NADPH oxidase components, which may exhibit residual catalytic function, a less aggressive disease and longer survival rates. According to data from reported cases of CGD in the United States, mutations in p47^{phox} account for around 25% of CGD cases, whilst p22^{phox} and gp67^{phox} are responsible for around 5% of cases each (Song *et al.*, 2011). However, incidences of X-linked and autosomal recessive CGD may be complicated by data published by Gutierrez *et al.* (2012) who published a case of X-linked CGD in a nine year old boy presenting with recurrent pneumonia. Interestingly, although the residual NADPH oxidase activity and isolated lung involvement suggested an autosomal recessive form of CGD, genetic testing revealed a single nucleotide mutation in exon 3 of the *CYBB* gene (substitution at 252 G>A). This X-variant mutation did not affect the amino acid sequence (Ala84Ala) but resulted in reduced catalytic activity of the NADPH oxidase complex and highlighted that even one type of CGD can present with a heterogeneous phenotype. This may suggests that other NADPH subunits may take over when its other subunits are mutated.

As indicated by the autosomal recessive cases of CGD, the cytosolic protein subunits play an important role in NADPH oxidase activation. The smallest of these proteins, p40^{phox}, is encoded by the *NCF4* (neutrophil cytosol factor 4) gene in humans (Zhan *et al.*, 1996), which binds with p47^{phox} and p67^{phox} in the cytosol to form a complex that further interacts with Rac1. Biochemical data suggest that these cytosolic protein subunits are required for gp91^{phox} (and therefore NADH oxidase) activation. The p47^{phox} domains are conserved to allow binding to both p67^{phox} and gp91^{phox}, and when

NADPH oxidase is in a resting state, these domains are sequestered to prevent enzyme activation (DeLeo *et al.*, 1996). Although the data from Song *et al.* (2011) highlighted that p47^{phox} mutations accounted for one quarter of CGD cases, experiments in mice conducted by Yi *et al.* (2012) found that animal survival rates of p47^{phox} mutants were similar to wild-type. The authors noted that these mutant strains produced higher concentrations of alternatively activated macrophages, which were able to produce ROS through a NADPH oxidase-independent mechanism, and resulted in enhanced production of cytokines. The concentration of ROS produced was comparable to NADPH oxidase and were able to mediate killing of *Listeria monocytogenes* bacteria *in vivo*.

Phosphorylation is the primary means of post-translational regulation of the NADPH oxidase subunits, with the addition of phosphate groups serving to both positively and negatively regulate NADPH activity. For example, the addition of phosphate groups to p40^{phox}, decreases overall NADPH oxidase activity, but phosphorylation of p47^{phox} after phagocytosis, serves to expose sequestered domains through a conformational change, allowing interaction with p67^{phox}. Data show that the phosphorylation of p47^{phox} coincides with the generation of ROS by stimulated polymorphonuclear leukocytes (DeLeo *et al*., 1999). Likewise, the termination of the respiratory burst correlated with the removal of p47^{phox} and p67^{phox} from the cell membrane and export from the macrophage phagosome. DeLeo *et al.*, (1999) conducted a series of experiments to examine the kinetics of protein subunit activation and concomitant ROS generation. The authors observed that the respiratory burst of superoxide occurred immediately after pathogen phagocytosis by polymorphonuclear leukocytes, but this activity declined soon after engulfment.

It should be noted that, in addition to the NADPH oxidase system, there are other mechanisms to generate ROS, which may mean that mutations in the protein subunits may not necessarily result in CGD. For example, xanthine oxidase, involved in purine metabolism, is able to generate O_2^- as part of a host defence against invading microbial pathogens. This mechanism is essential for host defence in NADPH oxidase-deficient mice, but is dispensable in wild-type mice (Segal *et al.*, 2000b). In addition, normal mitochondrial respiration can produce ROS for use in the host defence. West *et al.* (2011) demonstrated that specific toll-like receptors (TLR) in macrophages recruit mitochondria to phagosomes so that the metabolic production of ROS can target intracellular bacteria. In addition to direct antimicrobial activity, NADPH oxidase activation in neutrophils is linked to the extracellular release of granule proteins, DNA and chromatin, which aggregate to form neutrophil extracellular 'traps' that bind and kill bacteria (Brinkmann *et al.*, 2004) and fungi (Bianchi *et al.*, 2009; Urban *et al.*, 2006).

1.6 Macrophages, cytokines and NADPH

As part of the immune response in humans, phagocytic cells, including polymorphonuclear leukocytes (PML), monocytes and macrophages are recruited to sites of infection. Monocyte/Macrophage recruitment depends on the detection of molecules present in the debris of necrotic cells. These molecules are identified through toll-like receptors (TLRs) and the interleukin-1 receptor (IL-1R) (West *et al*., 2011). Stimulation of macrophages occurs in animal models that do not have lymphocytes, suggesting that the process does not rely on the presence of an adaptive immune response (Mosser and Edwards, 2008,).

Macrophages are present in virtually all tissues in the body and they form part of the innate and adaptive immune response, engulfing (phagocytosing) cellular debris and pathogens and killing them via an oxidative burst generated primarily by NADPH oxidase, as discussed. In humans macrophages are recognised in the immune system by the expression of several proteins, including CD14, CD40, CD11b, CD64, EMR1, and importantly, the membrane-degrading enzyme, lysozyme (Mosser and Edwards, 2008). During phagocytosis, the pathogen becomes engulfed within the phagosome, a vacuole which fuses with the macrophage lysosome. Within the phagolysosome a combination of ROS and degrading enzymes combine to digest the pathogen. In addition to this direct pathogen killing function, macrophages 'present' antigens from digested pathogens to helper T cells of the adaptive immune system. This presentation is performed by integrating the antigen into the macrophage cell membrane and attaching it to an MHC class II molecule that prevents the macrophage from being recognised by other immune cells as a pathogen. Furthermore, macrophages produce complement proteins and regulatory factors, including interleukin-1 (IL-1), and tumour necrosis factor (TNFα) cytokines involved in the production of the inflammatory immune response. TNFα encoded by *TNFA* on chromosome 6p21.3, is an important macromolecule in the regulation and recruitment of immune cells, such as neutrophils, and the cytokine promotes the expression of adhesion molecules on endothelial cells, allowing neurophils to migrate to sites of infection. TNFa also stimulates the process of phagocytosis, and the production of IL-1 (which is IL-1a and IL-1b). interleukin-1β (IL-1β), encoded by *IL1B* (Auron *et al.*, 2007), initiates an intracellular signalling cascade that leads to the activation of transcription factors (e.g. is NF-κB) and the expression of target

genes, some of which are involved in the production of ROS. For example, in monocytic cells, IL-1β leads to the production of ROS through a process that required NADPH oxidase activity (Bonizzi *et al.*, 1999). According to the authors, this pathway involved the translocation Rac1 GTPase and is likely to follow the NADPH oxidase activation process, outlined in Figure 1.

Importantly for the present study, mutations in TNFa and IL-1 receptors have been associated with CGD (Kang *et al*., 2011,), confirming results by Bonizzi *et al*. (1999) that established a link between these cytokines and NADPH activation. Furthermore, insufficient regulation of inflammation by cytokines may result in autoimmune complications in patients with CGD. It has been shown previously that inflammatory complications and autoimmune problems may develop in patients with CGD (De Ravin *et al.*, 2008) as macrophage clearance of apoptotic cells relies on the activity of NADPH oxidase.

It is possible to block TNFa-mediated inflammation in human cells using an inhibitor, such as the monoclonal antibody, infliximab (Kang *et al*., 2011), however cases published by Uzel *et al.* (2010) identified that TNF neutralisation was potentially dangerous in patients with CGD, as the cytokine acts to decrease susceptibility to subsequent pathogen infection.

Attenuated macrophage activity results in impaired clearance of antigens, continued recruitment of neutrophils and prolonged activity of pro-inflammatory cytokines, as reported in cases of X-linked CGD (Gallin and Buescher, 1983). Taken together, these reports suggest a much broader role for NADPH oxidase than simply production of ROS, instead highlighting an important role in the enzyme in cellular signalling and recruitment of aspects of both the innate and adaptive immune system. The multifaceted nature of NADPH oxidase regulation helps to explain the phenotypic heterogeneity of CGD, with a different genetic mutations resulting in altered expression of NADPH oxidase and different concentrations of ROS.

The oxidative burst generated by phagocytes is produced by ROS through the action of NADPH oxidase. ROS has also been implicated in the activation of the NLRP3/NALP3 inflammasome during pathogen invasion (Martinon *et al*.; 1999). Inflammasones induce the release of inflammatory caspases such as caspase-1, which trigger further inflammation via the release of cytokines including IL-1β. In monocytes derived from CGD patients, there was found to be a high level of caspase-1 and subsequently IL-1β signalling, indicative of an excessive inflammasone activation (van de Veerdonk *et al*.; 2009). ROS additionally contributes to TLR4 signalling via its ability to activate the transcription factors for the inflammatory regulators NFκB and AP-1, as well as inducing cytokine release (Asehnoune *et al*.; 2004).

Chapter 2

2.0 Aims

This dissertation aims to perform a detailed study to assess the following hypothesis:

Different mutations in the subunits of NADPH oxidase (gp91^{phox}, p22^{phox}, p40^{phox}, p47^{phox}, p67^{phox}) result in an altered macrophage response to infection.

The formulation of this hypothesis was based on findings from the scientific literature, which identified mutations in genes encoding the NADPH subunits, resulted in altered abilities of host cells to produce ROS, which in turn manifested as different forms of CGD. The study by Yi *et al*. (2012) was particularly intriguing in this regard, revealing that mutations in p47^{phox} resulted in a different mechanism of ROS production through alternatively activated macrophages. This mechanism had a bactericidal effect on *L. monocytogenes*, and it will be interested to observe in future whether the altered production of interleukin has an effect on tissue inflammation and the immune system, as observed previous in patients with CGD (De Ravin *et al*., 2008).

It is envisaged that, in line with previous studies (for example, Bjorgvinsdottir *et al*., 1996) mutations in *CYBB*, encoding gp91^{phox} will lead to decreased ROS production through NADPH oxidase. Inheritance of this mutated gene is responsible for the X-linked form of CGD, which shows dramatically decreased production of ROS and susceptibility to microbial pathogens.

Mutations in genes encoding other NADPH oxidase subunits (e.g. *CYBA*) are expected to show attenuated production of ROS, however the concentration of the superoxide anion in the macrophage phagosome is expected to be sufficient to have an antimicrobial effect, especially if NADPH activity is augmented by recruitment of ROS from other sources, such as from mitochondria recruited to the macrophage phagosome by toll-like receptors (West *et al.*, 2011).

This study will investigate the production of important inflammatory cytokines in human macrophages in which the expression of different NADPH oxidase subunits have been mutated. The aims are

1) Develop a Human macrophage model in which to investigate TNFa & IL-1b expression after TLR4 and inflammasomme activation.
2) Investigate the effect of p47phox and gp91phox inhibition in these models
3) Investigate the effect of TSPO18 (protein we had previously shown to be inhibited in NADPH oxidase deficient cells.) inhibition in this model.

The present study will add to the body of scientific literature that exists on the structure

of the NADPH oxidase and the mutagenic approach devised is designed to further the understanding of how the structure of this important enzyme impacts on the activity of the immune system in general, and macrophages in particular. In the longer term, it is hoped that outcomes from this work may inform future therapeutic intervention strategies to combat chronic granulomatous disease.

Chapter 3

3.0 Materials and methods:

This section will outline the techniques and reagents used to perform the experiments described in this study. All chemicals used were of laboratory grade; unless otherwise stated; and were primarily supplied by Invitrogen Life Sciences (Paisley; UK). When other suppliers were used; they have been noted in this section. All reagents and buffers were stored at 2-8°C for a maximum of one week to ensure full activity. All plastic and glassware were of laboratory standard and were sterilised prior to use.

3.1 Culture Medium

Roswell Park Memorial Institute (RPMI)-1640 culture medium (Sigma; UK) was used to store and propagate cells used in this study. As indicated; the cell culture medium was occasionally supplemented with 10% foetal calf serum (InvivoGen; UK); as well as the antibiotics streptomycin and penicillin (both Sigma; UK).

3.2 Cell culture and *in vitro* treatment

Cell culture experiments were performed on U937 cells; a model cell line isolated from a histiocytic lymphoma (Lehmann; 1998). Upon maturation; U937 cells adopt the characteristics of mature macrophages; including the production of cytokines; and are therefore an ideal model for the *in vitro* study of the immune response.

For the experiments described in the present study; U937 cells were stored in RPMI-1640 medium (Invitrogen; Paisley; UK); supplemented with 10% foetal bovine serum (FBS); penicillin (100 U/ml) and streptomycin (100 µg/ml). Three sources of U937 cells (referred as A; B and C) were cultured in an incubator maintained at 37ºC with an atmosphere of 95%:5% (O_2:CO_2). U937 cells were cultured for two to three weeks until they reached exponential phase of growth. After incubation; culture flasks were carefully scraped to remove cells that had adhered to the surface of the flask. The cells were then placed into a container containing fresh RPMI medium; centrifuged and counted using a haemocytometer. The Trypan Blue vital stain (0.4%) was used to quantify the number of dead cells; which were subsequently eliminated from the total cell count to give the total viable cell concentration. After the viable cells had been quantified; the culture was added to each well of a 24-well plate at a concentration of 2×10^5 cells/ml. The plates were then incubated for at least 24 hours before testing; to allow the cells to recover. The remaining cell solution was passaged by transfer to a new square-bottomed flask and fresh RPMI-1640 medium was added.

After the U937 cells had reached mid-exponential phase of growth; they were treated with three different concentrations (1; 3 or 10 pg/ml) of phorbol-12-myristate-13-acetate (PMA) to induce monocyte differentiation into macrophages; which has been outlined previously (Daigneault *et al.*; 2010). Cells were left for up to 3 days so that they could adhere to the tissue culture plate. At the end of the incubation period; the cells were washed once with 1 ml of RPMI-1640 tissue medium culture to remove excess cell debris.

3.3 Monosodium urate (MSU) preparation

The uric acid crystals; present in MSU are regarded as an important factor for activating inflammation and the immune response. This is due to the induction by MSU of phagocytosis and cytokine production (reviewed by Shi *et al.* (2010). The following method describes the formation of MSU from uric acid.

1.68g of uric acid was added to 10 µM NaOH and heated to 70°C. NaOH/HCl was added drop-wise to maintain the pH range between 7.1 and 7.2. The solution was stirred slowly and continuously at room temperature for 24 hours. MSU crystals were harvested after decanting the supernatant. The crystals were washed; dried and dispensed into individual vials (10 mg); and sterilised by autoclaving. The needle shape and size of the crystals were verified via polarising light microscopy (Galvez *et al.*; 2002). After formation; the sterile MSU crystals were resuspended in RPMI-1640 medium and diluted to an appropriate final concentration for activating the U937 macrophages.

3.4 ELISA

The level of TNFα was determined in the supernatants of U937 cell cultures using a sandwich enzyme-linked immunosorbent assay (ELISA) technique (Lequin; 2005). For the experiments outlined here; the ELISA protocol was taken from *Gen-Probe Diaclone Human TNFα Kit* and followed according to manufacturer's instructions.

Preparation of ELISA plates

Briefly; 100µl of a specific capture antibody was mixed with 10 ml of a coating buffer (1×PBS; pH 7.2-7.4) and used to coat the wells of a microtitre strip plate. The plate was incubated overnight at 4°C and any uncoated antibody was removed by adding 2×0.4 ml wash buffer

(1×PBS; 0.05% Tween20). Next; 0.25 ml blocking buffer (1×PBS; 5% BSA) was added to each well and the plate was incubated at room temperature for two hours. A second wash step was performed with 3×0.4 ml wash buffer.

3.5 Quantifying the concentration of TNFα and of IL-1β protein

Depending on the experiment; either TNFα or IL-1β protein was added to the coated and blocked plates; and left to bind to the corresponding antibody. Any unbound protein removed by a washing step as described previously. A second; biotinylated antibody was reconstituted with a Reconstitution Buffer (1×PBS; 0.09% Azide) and then added along with 0.1 ml of a Streptavidin-horseradish peroxidase (HRP) conjugate (Invitrogen; Paisley; UK) (Cartun and Pedersen; 1989). The plates were incubated for 30 minutes at room temperature and after a further wash step; 0.1 ml of a ready-to-use TMB chromogenic substrate was added (Josephy *et al.*; 1982). The plates were incubated in the dark for 5-15 minutes before 0.1 ml of Stop Reagent was added (1M sulphuric acid) and the absorbance recorded on an ELISA Plate Reader (Bio-Tek; Bedfordshire; UK) at 450 nm.

The intensity of the chromogenic substrate-mediated colour change is proportional to the concentration of antibody-bound protein. The colour intensity was compared with a standard curve of known TNFα concentrations (12.5; 25; 50; 100; 200; 400 and 800pg/ml) to accurately calculate the amount of protein present.

The ELISA method outlined here for TNFα was repeated for IL-1β; using a specific antibody and the absorbance compared with a separate standard curve of known IL-1β concentrations (7.8; 15.6; 31.3; 62.5; 125; 250 and 500pg/ml). Each standard and sample was pipetted into the plate twice; creating a duplicate of each sample. For clarity; an example plate layout can be found in the *Appendix*.

3.6 MTT assay

In some experiments; loss of U937cell viability may impact on the reliability of the results. To confirm cell viability; a 3-(4,5-dimethylthiazol-2-yl)-2,5-diphenyltetrazolium bromide (MTT) assay was used. The assay relies on a colorimetric change of the tetrazolium dye; MTT; from yellow to purple after reduction by NADPH-dependent cellular oxidoreductase enzymes (van Meerloo *et al.*; 2011). The resulting product; formazan blue, can be detected by a spectrophotometric absorbance at a wavelength of 500-600nm. For the cell viability experiments conducted; the MTT method was applied as follows:

After 20 hours of incubation; unattached U937 macrophages were removed with wash steps using 300µl of warm PBS. The viability of attached U937 macrophages was evaluated by using FCS-free culture medium containing 5 mg/ml MTT (Sigma-Aldrich; UK). After 20-30 minutes of incubation at 37°C; the culture medium was discarded. The resulting formazan blue was dissolved with 300µl DMSO and its optical density was measured at 540nm. Any intrinsic background signal from negative control samples was subtracted from the absorbance readings obtained from each sample.

Lipopolysaccharide (LPS) is one of the major constituents of Gram-negative bacteria and has been shown previously to cause macrophage killing *in vitro* by inducing nitric oxide production and the subsequent formation of the cytotoxic superoxide anion (Kim and Ha; 2009). LPS was used in the present study to confirm macrophage cytotoxicity and to standardise the MTT assay. Ultra-pure LPS derived from *Escherichia coli* 0111:B4 (Invivogen; UK) was dissolved in phosphate-buffered saline (PBS) and used at a final concentration of 5 mg/ml.

For calculating the relative viability; control cells; in which no LPS had been added; were tested by the MTT assay. The mean absorbance readings from control cells were assumed to represent 100% viability so that the relative viability (%) from samples could be calculated as follows:

(OD of experimental sample/OD of the control cells) × 100.

3.7 RNA Interference (RNAi)

The Phox subunits $p47^{phox}$; $gp91^{phox}$ and PBR (U937 cell source A) were selected to undergo RNAi as they achieved the best IL-1β response to MSU treatment. Firstly; the U937 cells were differentiated into macrophages by the addition of 10ng/ml PMA. Following this; the siRNA protocol was carried out as follows:

The differentiated U937 cells were transfected by incubating 150nM of $p47^{phox}$ siRNA duplex; $gp91^{phox}$ siRNA duplex; PBR siRNA duplex or scrambled siRNA duplex control (Qiagen Ltd) in FBS-free RPMI containing 0.8% oligofectamine (Invitrogen) for 3 hours. Cells were then returned to normal conditions for 48 hours.

After this time the cells were assayed for IL-1β and TNFα production. Cells were stimulated with 100units/ml of LPS for 18 hours (medium removed and assayed for IL-1β and TNFα) followed by 4 hours of MSU treatment (medium removed and assayed for IL-1β). The MTT assay was carried out on cells at the end of the MSU treatment to assess cell viability.

The siRNA target sequences were designed using Ambion software and subjected to blast search (NCBI database) against human EST to ensure selectivity of target sequences. The sequences were as follows:

- $p47^{phox}$ target sequence: AACTATGCAGGTGAGCCATAC;
- $gp91^{phox}$ target sequence aatggtgtgtgaatgcccgag;
- PBR target sequence tCCATGGCTGGCATGGGGGA.

3.8 Statistical analyses

The TNFα and IL-1β ELISA experiments were carried out in duplicate and the data were subsequently analysed. The standard error of the mean (SEM) of the results were obtained and comparisons between groups were performed using a one-way analysis of variance (ANOVA) test (Gelman; 2005); followed by a student's *t*-test; with a value of $P < 0.05$ considered as statistically significant.

To calculate the TNFα release concentration the absorbance values for the known standard concentrations were compared with the absorbance data for each sample. To identify the mean calculated TNFα release for each treatment group; the absorbance value for each sample was analysed individually and averaged with the other samples from the same group (n=4).

The data analysis for the release value was performed using Prism software (GraphPad). All subsequent analyses were performed out using Excel (Microsoft Corporation).

Chapter 4

4.0 Results

4.1 MTT Assay

Colony A (treated for 4 hours with LPS)

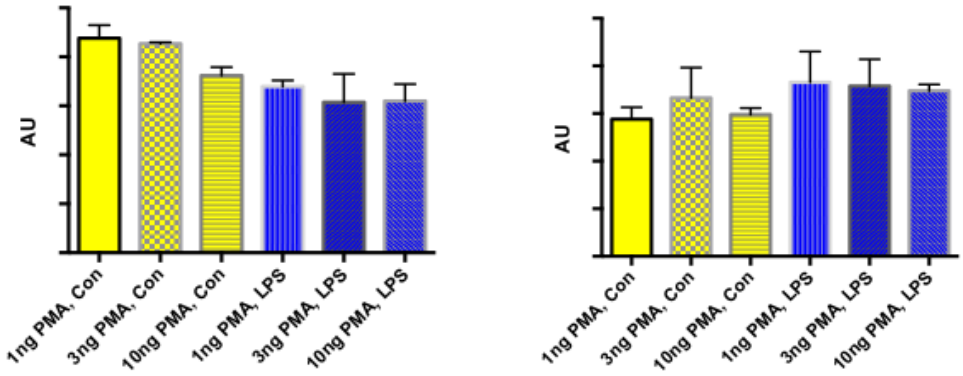

24hours 72hours

(Fig 2.10) MTT assay on PMA Differentiated U937 (Colony A). U937 cells were differentiated for 24 hours/72 hours with indicated concentrations of PMA (1; 3;10ng/ml); washed and treated for 4 hours with medium (Con) or LPS (100U/ml).

At 24 hour differentiation; the two-way ANOVA shows that both the row factors (differences between the x values/effect of LPS and PMA concentration) and column factors (differences between the y values/AU measurements) are not significant; meaning that the data cannot be analyzed.
At 72 hour differentiation; the two–way ANOVA shows that the row factor is not significant but the column factor is significant ($p<0.0001$); meaning that the AU values obtained are statistically significant. In the LPS-activated group; the mean AU values obtained were higher than the control group. A small drop in the AU levels can be seen in the LPS-treated group in response to an increasing PMA concentration. This trend is not apparent in the control group.

Colony A (treated for 24 hours with LPS)

24hours 72hours

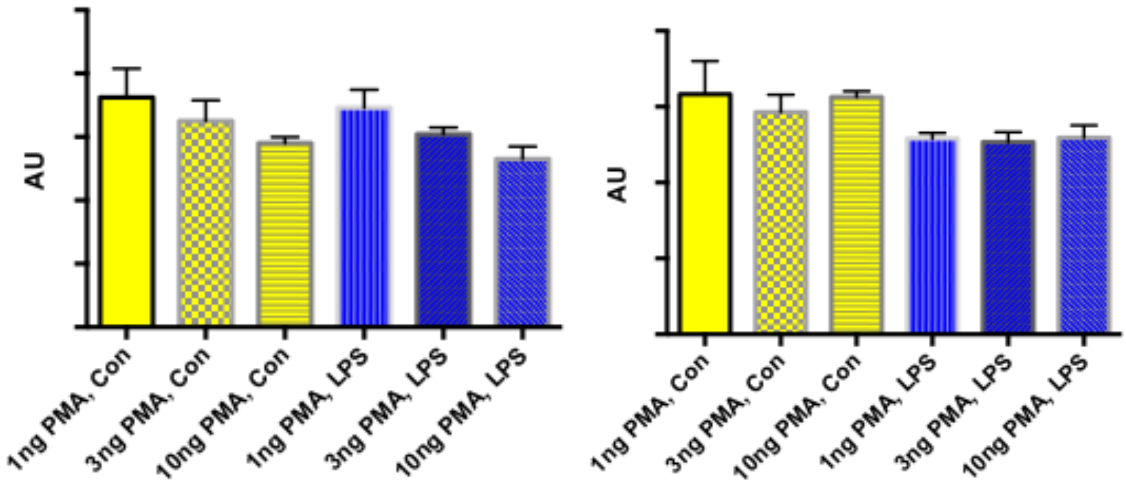

(Fig 2.11) MTT assay on PMA Differentiated U937 (Colony A)

At 24 hour differentiation; the two–way ANOVA concludes that the row factor is not significant but the column factor is significant ($p<0.0022$). A general trend is evident in both the control and LPS-treated groups- as the PMA concentration increases; the AU reading decreases in a step-wise manner. A small difference in AU levels exists between the control and LPS-treated groups; with slightly higher levels witnessed in the control group.
At 72 hour differentiation; the two-way ANOVA shows that both the row factor and column factor are not significant therefore the data cannot be analyzed.

Colony B (treated for 4 hours with LPS)

24hours 72hours

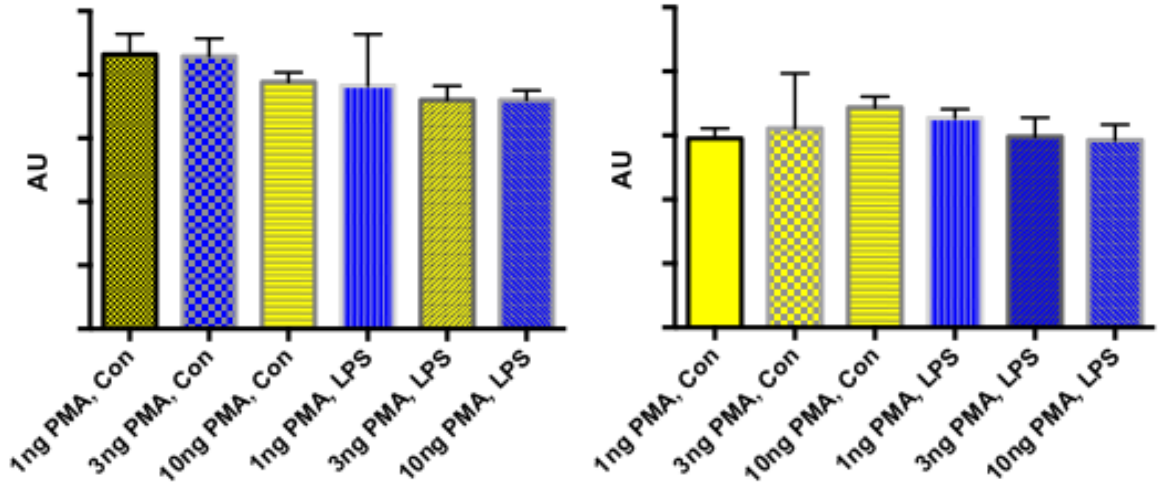

(Fig 2.12) MTT assay on PMA Differentiated U937 (Colony B)

At both 24 and 72-hour differentiations; the two-way ANOVAs indicate that the row factors and column factors were not significant for either group; meaning the data cannot be accurately interpreted.

Colony B (treated for 24 hours with LPS)

24hours 72hours

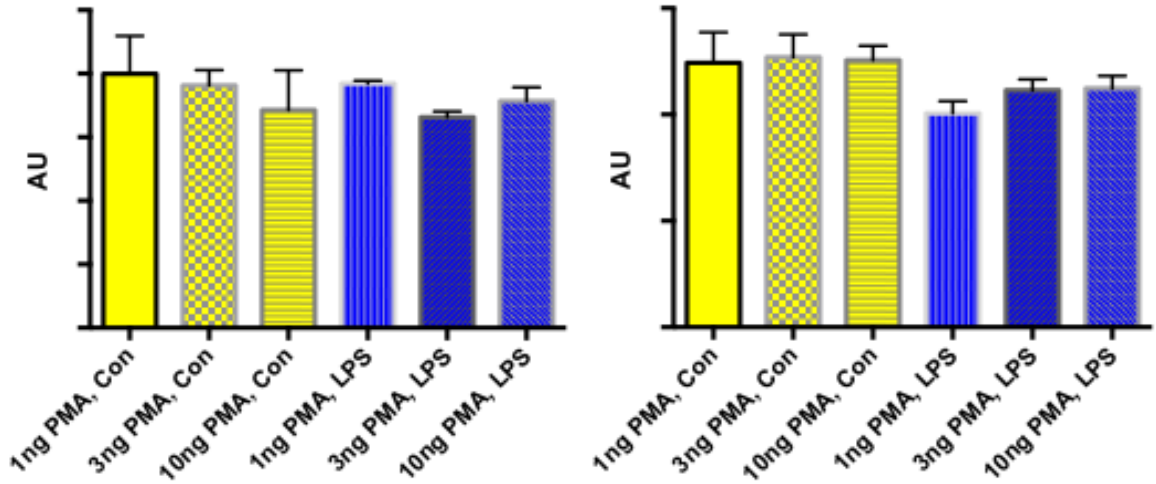

(Fig 2.13) MTT assay on PMA Differentiated U937 (Colony B)

At 24 hour differentiation; the two–way ANOVA shows that the row factor is not significant but column factor is highly significant ($p<0.0006$). Minor differences in the AU levels are apparent between the control and LPS-stimulated groups. A similar trend to that seen in Figure 2.11 can also be observed here; as the concentration of PMA rises in the control and LPS-treated groups; the AU values decrease accordingly.

At 72 hour differentiation; the two–way ANOVA shows that both the row factor ($p<0.0024$) and the column factor ($p<0.0001$) are significant. From the graph we can see that AU readings are lowest in the LPS-treated group. Minimal differences in the AU readings exist between each concentration of PMA in the LPS-treated group and also in the control group.

Colony C (treated for 4 hours with LPS)

24hours 72hours

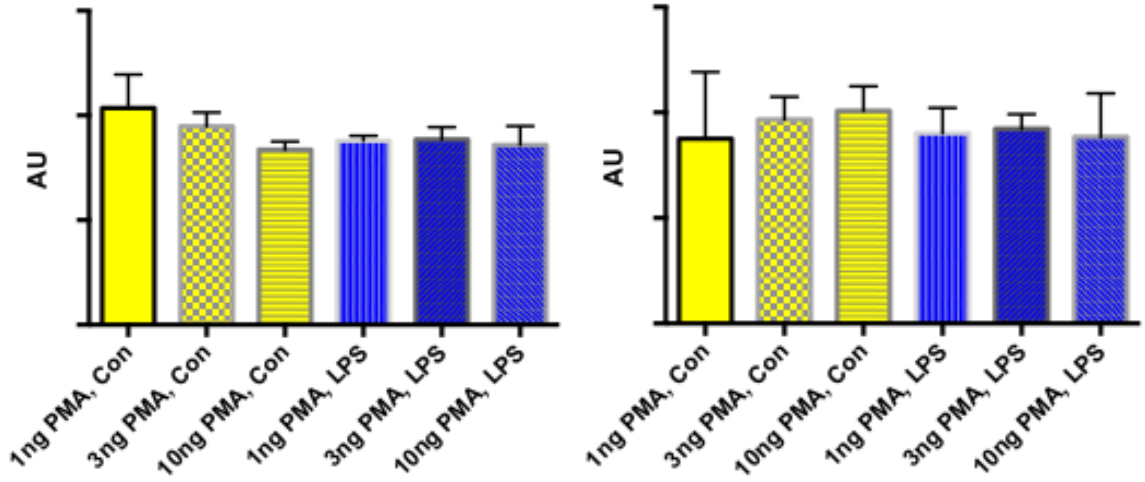

(Fig 2.14) MTT assay on PMA Differentiated U937 (Colony C).

In both the 24 and 72 hour differentiation groups; the two-way ANOVAs show that the row factors and column factors were not significant in either group meaning the data cannot be evaluated.

Colony C (treated for 24 hours with LPS)

24 hours 72hours

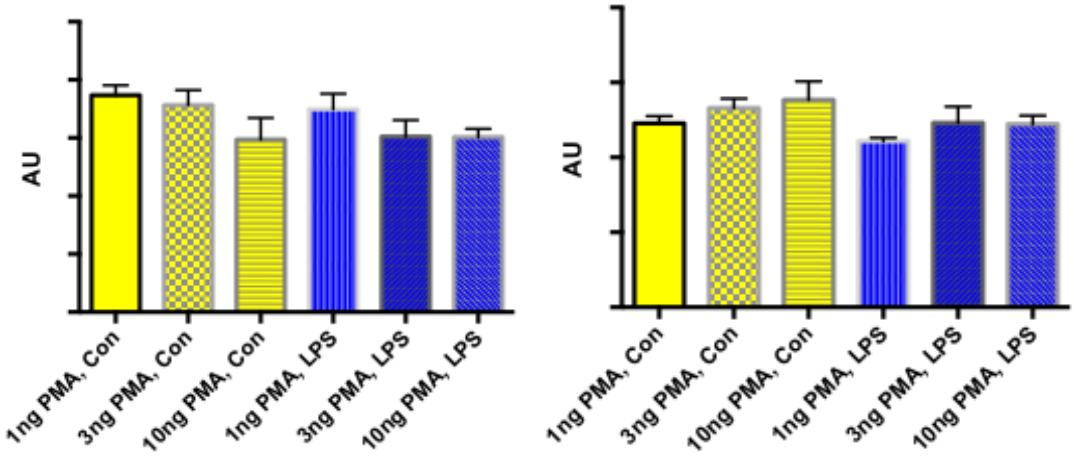

(Fig 2.15) MTT assay on PMA Differentiated U937 (Colony C)

At 24-hour differentiation; the two–way ANOVA shows that the row factor is not significant and the column factor is significant ($p<0.0038$). The general trend appearing in both the control and LPS-treated groups is that as the concentration of PMA rises; the AU value lowers in turn. Comparable levels are observed between the two experimental groups.

At 72 hour differentiation; the two–way ANOVA shows that the row factor is not significant but the column factor is significant ($p<0.0017$). As the PMA concentration increases; the AU values increase; contrasting with previous findings. The AU values were highest in the control group in comparison to the LPS-treated group.

4.2 Colony A; TNFα and IL-1β analysis

TNFα; 24 hours differentiation

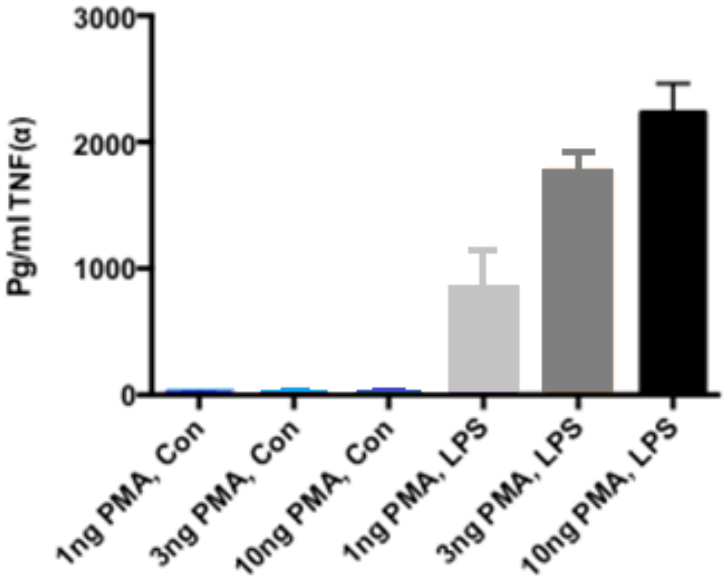

(Fig 3.10) TNFα assay on 1 day PMA Differentiated U937 (Colony A). U937 cells were differentiated for 24 hours with indicated concentrations of PMA (1; 3;10ng/ml); washed and treated for 4 hours with medium (Con) or LPS (100U/ml).

None of the control readings were statistically significantly. However; significant results were obtained in the LPS-stimulated cells; a dose-related increase in TNFα production was seen in accordance with the PMA concentration.

Control	LPS	Con x LPS
1ng x 3ng = ns	1ng x 3ng = yes; 0.0104	1ng x 1ng = yes; 0.0130
1ng x 10ng= ns	1ng x 10ng= yes; 0.0037	3ng x 3ng= yes; 0.0001
3ng x 10ng= ns	3ng x 10ng= ns	10ng x 10ng= yes; 0.0001

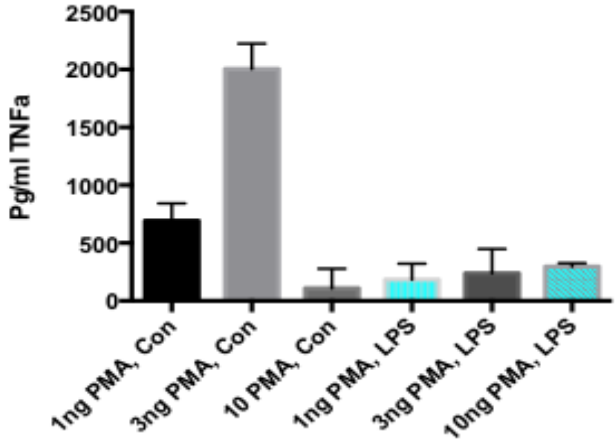

(Fig 3.11) TNFα assay on 1 day PMA Differentiated U937 (Colony A).

In the LPS-treated group; a dose-related increase in TNFα production can be observed; corresponding to the PMA concentration. The results of the control groups were significant; with an extremely high TNFα production at 3ng PMA. The levels of TNFα produced by the LPS-treated group were significantly less than the levels induced by the control group (with the possible exception of the 10ng PMA control group).

Control	LPS	Con x LPS
1ng x 3ng = yes; 0.0001	1ng x 3ng = ns	1ng x 1ng = yes; 0.0025
1ng x 10ng= yes; 0.0022	1ng x 10ng= ns	3ng x 3ng= yes; 0.0001
3ng x 10ng= yes; 0.0001	3ng x 10ng=ns	10ng x 10ng= ns

TNFα; 72 hours differentiation

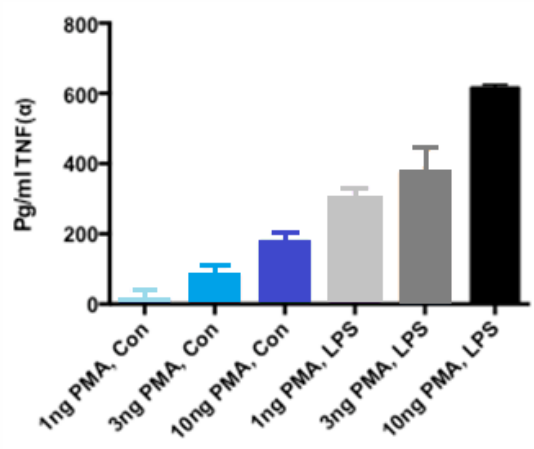

(Fig 3.12) TNFα assay on 3 days PMA Differentiated U937 (Colony A).

The readings obtained for LPS stimulation at each concentration of PMA were statistically significant; versus the control. The apparent trend is that as the PMA concentration increases; the corresponding levels of TNFα increase in response. A similar trend was seen in the control cells. However; higher TNFα levels were observed in the LPS-treated groups in comparison with the controls. Compared to 24 hour differentiation; the longer the exposure to PMA; the greater amounts of TNFα generated.

Control	LPS	Con x LPS
1ng x 3ng = ns	1ng x 3ng = ns	1ng x 1ng = yes; 0.0002
1ng x 10ng= yes; 0.0012	1ng x 10ng= yes; 0.0010	3ng x 3ng= yes; 0.0024
3ng x 10ng= yes; 0.0126	3ng x 10ng= yes; 0.0180	10ng x 10ng= yes; 0.0002

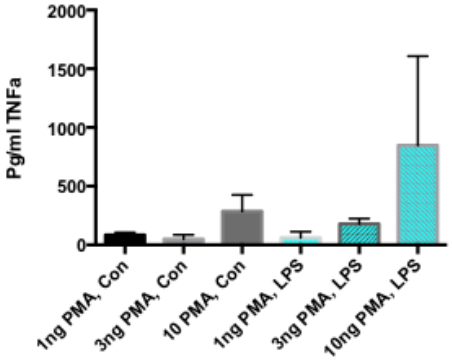

(Fig 3.13) TNFα assay on 3 days PMA Differentiated U937 (Colony A)

In the control group; significant readings were obtained for the 3ng and 10ng PMA groups; with a step-wise increase in TNFα production seen alongside an increase in PMA concentration. This confirms the findings of figure 3.12. With reference to the TNFα readings generated by the LPS-stimulated cells; the only significant reading obtained was at 3ng PMA and in comparison to the control group we can see that higher levels of TNFα are generated following LPS stimulation.

Control	LPS	Con x LPS
1ng x 3ng = ns	1ng x 3ng = yes; 0.0127	1ng x 1ng = ns
1ng x 10ng= yes; 0.0291	1ng x 10ng= ns	3ng x 3ng= yes; 0.0035
3ng x 10ng= yes; 0.0163	3ng x 10ng= ns	10ng x 10ng= ns

IL-1β; 24 hours differentiation

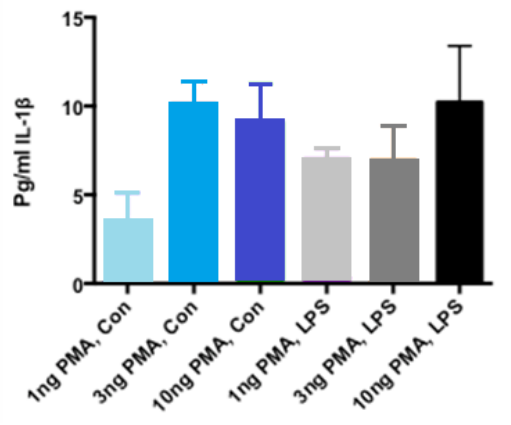

(Fig 3.14) IL-1β assay on 1 day PMA Differentiated U937 (Colony A).

This graph illustrates that higher concentrations of PMA induce higher levels of IL-1β. This is also demonstrated in the control group. Higher levels of IL-1β are seen in the LPS-treated groups (cells treated with 1ng PMA produced the only significant results) when compared to the controls.

Control	LPS	Con x LPS
1ng x 3ng = yes; 0.0006	1ng x 3ng = ns	1ng x 1ng = yes; 0.0066
1ng x 10ng= yes; 0.0061	1ng x 10ng= ns	3ng x 3ng= ns
3ng x 10ng= ns	3ng x 10ng= ns	10ng x 10ng= ns

IL-1β; 72 hour differentiation

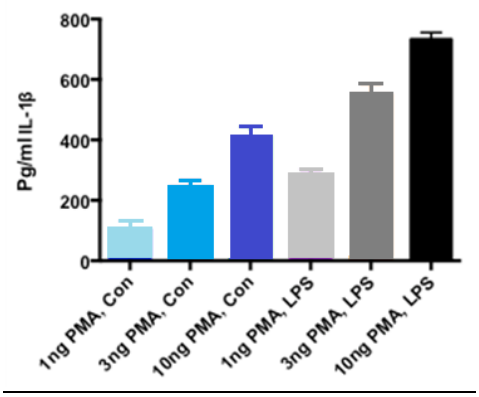

(Fig 3.15) IL-1β assay on 3 days PMA Differentiated U937 (Colony A).

Significant readings were obtained for the controls and LPS-stimulated cells at each concentration of PMA. The observed trend is that as PMA concentration increases; the IL-1β levels increase in accordance. Levels of IL-1β were highest in cells left to differentiate for 72 hours when compared to a 24 hour differentiation. A similar trend was seen in the control cells where LPS was not used. However; higher IL-1β levels were observed in the LPS-treated groups in comparison with the controls.

Control	LPS	Con x LPS
1ng x 3ng = yes; 0.0002	1ng x 3ng = yes; 0.0001	1ng x 1ng = yes; 0.0001
1ng x 10ng= yes; 0.0001	1ng x 10ng= yes; 0.0001	3ng x 3ng= yes; 0.0001
3ng x 10ng= yes; 0.0001	3ng x 10ng= yes; 0.0001	10ng x 10ng= yes; 0.0001

IL-1β; 18 hours differentiation; no treatment with MSU

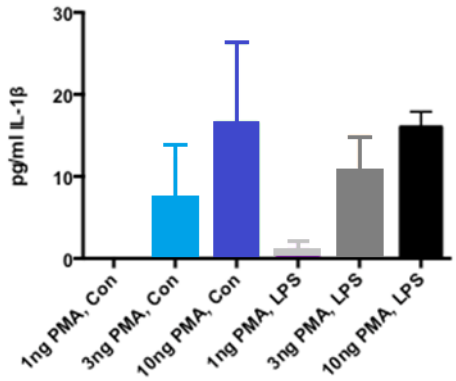

(Fig 3.16) IL-1β assay on 3 days PMA Differentiated U937 (Colony A).

The readings obtained at 1ng and 3ng PMA with LPS showed statistical significance. Comparing them with each other; we can see that there is a jump in IL-1β production when the concentration of PMA rises to 3ng.

Control	LPS	Con x LPS
1ng x 3ng = ns	1ng x 3ng = yes; 0.0044	1ng x 1ng = ns
1ng x 10ng= yes; 0.0153	1ng x 10ng= yes; 0.0001	3ng x 3ng= ns
3ng x 10ng= ns	3ng x 10ng= ns	10ng x 10ng= ns

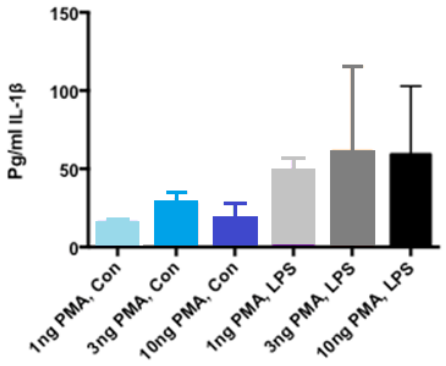

(Fig 3.17) IL-1β assay on 3 days PMA Differentiated U937 (Colony A).

P values calculated from this experiment were above the significance threshold; indicating that the results observed cannot be analysed and interpreted.

Control	LPS	Con x LPS
1ng x 3ng = ns	1ng x 3ng = ns	1ng x 1ng = yes; 0.0024
1ng x 10ng= ns	1ng x 10ng= ns	3ng x 3ng= ns
3ng x 10ng= ns	3ng x 10ng= ns	10ng x 10ng= ns

IL-1β; 18 hour differentiation with 4 hours treatment with MSU

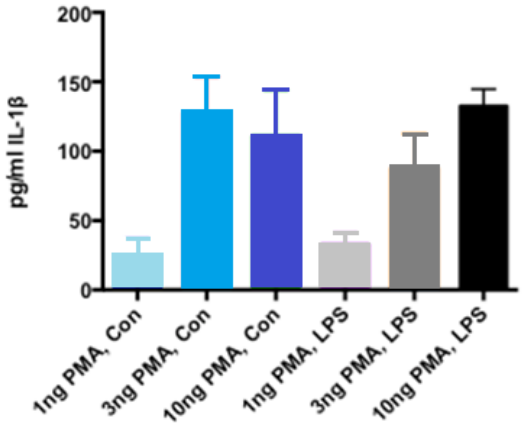

(Fig 3.18) IL-1β assay on 3 days PMA Differentiated U937 (Colony A) (MSU)

We can see a large jump in IL-1β production between the 1ng and 3ng PMA control groups; the only findings that proved to have statistical significance in the controls. We can also see the same trend in the LPS-treated group (all p

values were significant). However; comparison with the MSU-untreated group is difficult due to statistically insignificant results being obtained.

Control	LPS	Con x LPS
1ng x 3ng = yes; 0.0004	1ng x 3ng = yes; 0.0058	1ng x 1ng = ns
1ng x 10ng= yes; 0.0027	1ng x 10ng= yes; 0.0001	3ng x 3ng= ns
3ng x 10ng= ns	3ng x 10ng= yes; 0.0180	10ng x 10ng= ns

4.3 Colony A; RNA Interference

18 hours LPS stimulation; TNFα

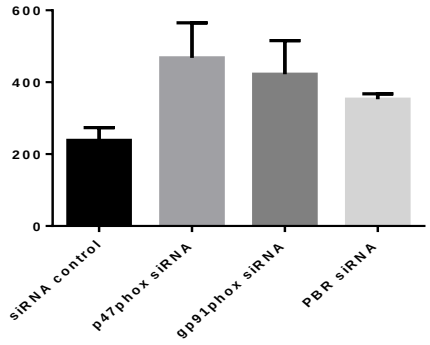

Statistically significant results were obtained for p47phoxsiRNA (p value 0.0045); gp91phoxsiRNA (p value 0.0102) and PBRsiRNA (p value 0.010) in comparison to the control group. P47phoxsiRNA generated the highest levels of TNFα relative to the control; followed by gp91phoxsiRNA and PBRsiRNA. The PBRsiRNA-treated cells had the lowest release of TNFα; however; levels were higher than that of the control. The column factor was significant (p value 0.0054)

18 hours LPS stimulation; IL-1β

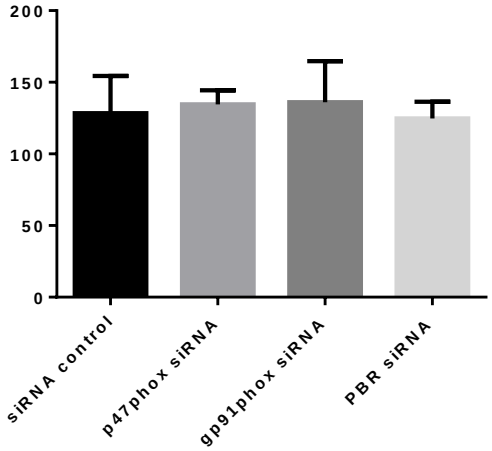

No statistically significant data was obtained from the two-way ANOVA. Both the row and column factors also proved to be insignificant.

18 hours LPS stimulation plus 4 hours MSU stimulation; IL-1β

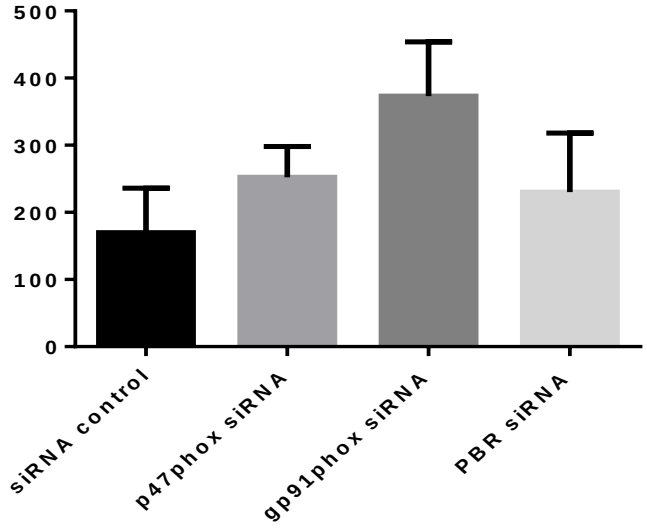

Statistically significant results were obtained when gp91phoxsiRNA was compared with siRNA control (p value 0.0081) and when it was compared with p47phoxsiRNA (p value 0.0403). The column factor can also be considered statistically significant; with a p value of 0.0382. Knock out of the gp91 subunit resulted in a substantial increase in IL-1β release when compared to the control. However; the effect of MSU on IL-1β production cannot be determined, as a comparison cannot be made with the previous graph due to the statistically insignificant results.

MTT graph

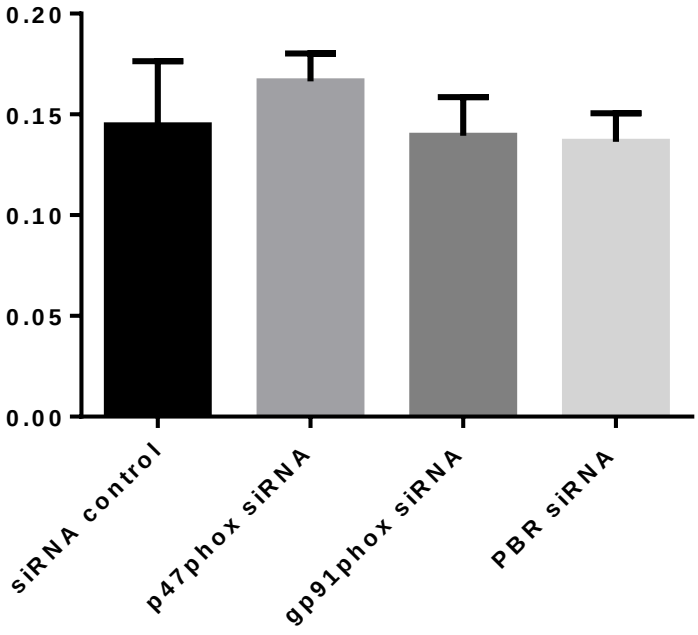

No significant results obtained.

4.4 Colony B; TNFα and IL-1β analysis

TNFα; 24 hours differentiation

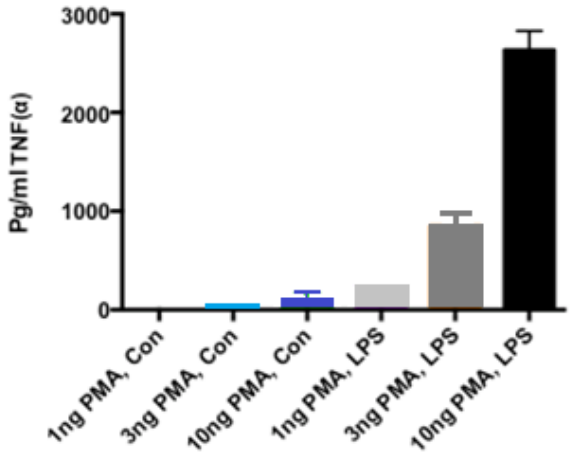

(Fig 4.10) TNFα assay on 1 day PMA Differentiated U937 (Colony B). U937 cells were differentiated for 24 hours with indicated concentrations of PMA (1; 3;10ng/ml); washed and treated for 4 hours with medium (Con) or LPS (100U/ml).

The readings obtained for the control group were not significant. However; this is not the case in the LPS-stimulated group and a concentration-related increase in TNFα production can be seen with reference to the PMA concentration.

Control	LPS	Con x LPS
1ng x 3ng = ns	1ng x 3ng = yes; 0.0008	1ng x 1ng = yes; 0.0001
1ng x 10ng= ns	1ng x 10ng= yes; 0.0001	3ng x 3ng= yes; 0.0002
3ng x 10ng= ns	3ng x 10ng= yes; 0.0002	10ng x 10ng= yes; 0.0001

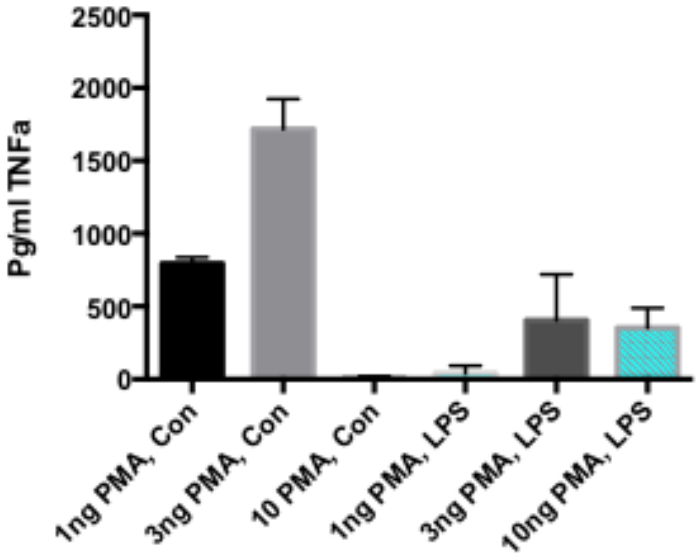

(Fig 4.11) TNFα assay on 1 day PMA Differentiated U937 (Colony B)

Both the control and LPS treated groups (relative to the control) yielded significant results. In the control group; a high level of TNFα was produced at the 3ng PMA concentration. Possibly related; a high level of TNFα was seen in the LPS-treated group at this PMA concentration but the reading was still lower than the control group. This was also observed with the 1ng group. The 3ng PMA LPS-stimulated group induced the highest levels of TNFα in the LPS treated group.

Control	LPS	Con x LPS
1ng x 3ng = yes; 0.0001	1ng x 3ng = ns	1ng x 1ng = yes; 0.0001
1ng x 10ng= yes; 0.0001	1ng x 10ng= yes; 0.0050	3ng x 3ng= yes; 0.0004
3ng x 10ng= yes; 0.0001	3ng x 10ng= ns	10ng x 10ng= yes; 0.0022

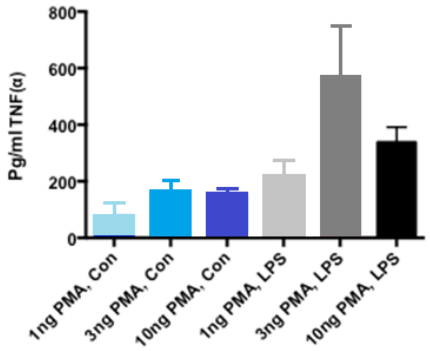

(Fig 4.12) TNFα assay on 1 day PMA Differentiated U937 (Colony B).

The readings of the control group were not statistically significant and will be discounted. The trend in the LPS-stimulated cells matches that seen in Figure 4.11; with the highest TNFα level produced in the cells treated with 3ng PMA.

Control	LPS	Con x LPS
1ng x 3ng = ns	1ng x 3ng = yes; 0.0140	1ng x 1ng = yes; 0.0065
1ng x 10ng= ns	1ng x 10ng= yes; 0.0331	3ng x 3ng= yes; 0.0205
3ng x 10ng= ns	3ng x 10ng= ns	10ng x 10ng= yes; 0.0048

TNFα; 72 hour differentiation

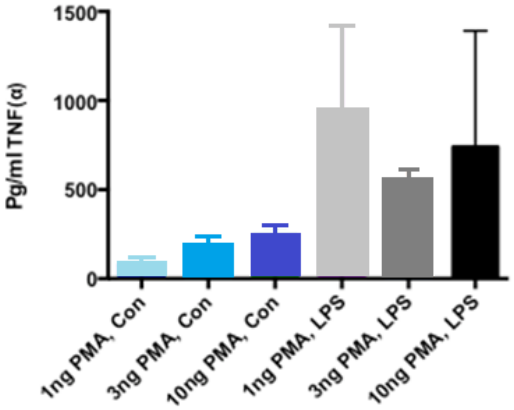

(Fig 4.13) TNFα assay on 3 days PMA Differentiated U937 (Colony B)

The LPS-treated; 3ng PMA group obtained a significant TNFα reading relative to the control.

Control	LPS	Con x LPS
1ng x 3ng = ns	1ng x 3ng = ns	1ng x 1ng = ns
1ng x 10ng= yes; 0.0064	1ng x 10ng= ns	3ng x 3ng= yes; 0.0019
3ng x 10ng= ns	3ng x 10ng= ns	10ng x 10ng= ns

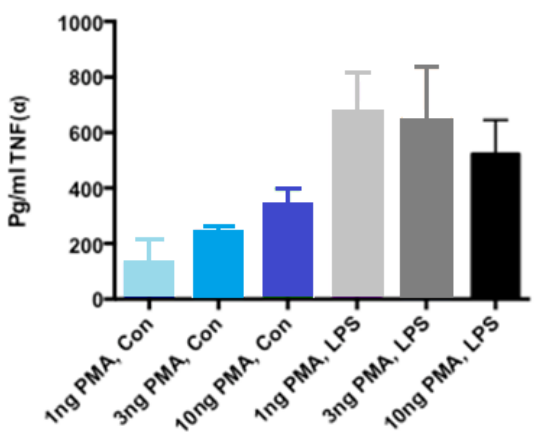

(Fig 4.14) TNFα assay on 3 days PMA Differentiated U937 (Colony B)

The LPS-treated; 3ng PMA group obtained a significant TNFα reading which was higher than its corresponding control group; as seen in figure 4.13. Similar levels of TNFα were seen in both the 1ng and 3ng PMA groups treated with LPS.

Control	LPS	Con x LPS
1ng x 3ng = ns	1ng x 3ng = ns	1ng x 1ng = yes; 0.0011
1ng x 10ng= yes; 0.0172	1ng x 10ng= ns	3ng x 3ng= yes; 0.0155
3ng x 10ng= ns	3ng x 10ng= ns	10ng x 10ng= ns

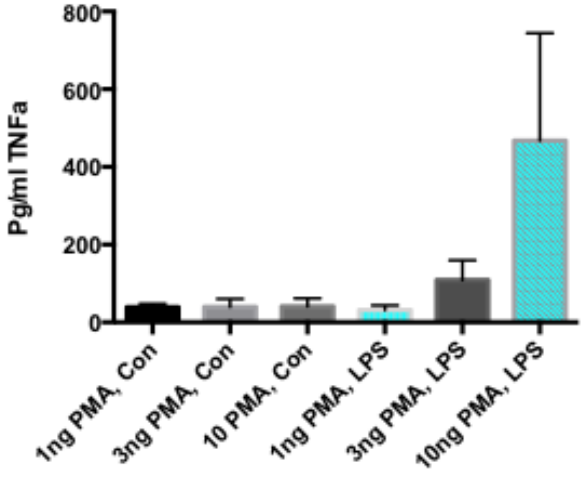

(Fig 4.15) TNFα assay on 3 days PMA Differentiated U937 (Colony B)

Statistically significant TNFα readings were obtained in the LPS-treated groups; and an increase in TNFα can be seen when there is a corresponding increase in PMA.

Control	LPS	Con x LPS
1ng x 3ng = ns	1ng x 3ng = yes; 0.0249	1ng x 1ng = ns
1ng x 10ng= ns	1ng x 10ng= yes; 0.0199	3ng x 3ng= yes; 0.0435
3ng x 10ng= ns	3ng x 10ng= yes; 0.0435	10ng x 10ng= yes; 0.0218

IL-1β; 24 hours differentiation

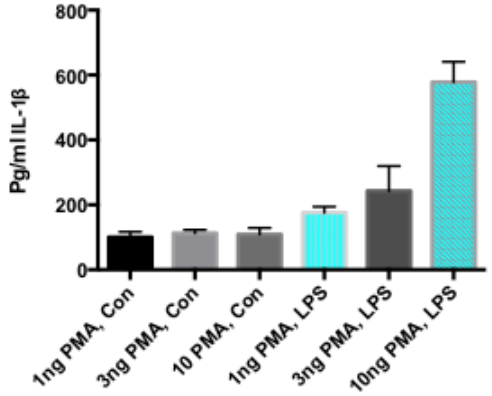

(Fig 4.16) IL-1β assay on 1 day PMA Differentiated U937 (Colony B)

The p values of the control groups are not considered to be significant. A general trend in IL-1β production; however; can be seen in the LPS-treated cells- as the PMA concentration increases the levels of IL-1β increase proportionately.

Control	LPS	Con x LPS
1ng x 3ng = ns	1ng x 3ng = ns	1ng x 1ng = yes; 0.0009
1ng x 10ng= ns	1ng x 10ng= yes; 0.0001	3ng x 3ng= yes; 0.0155
3ng x 10ng= ns	3ng x 10ng= yes; 0.0005	10ng x 10ng= yes; 0.0001

IL-1β; 72 hour differentiation

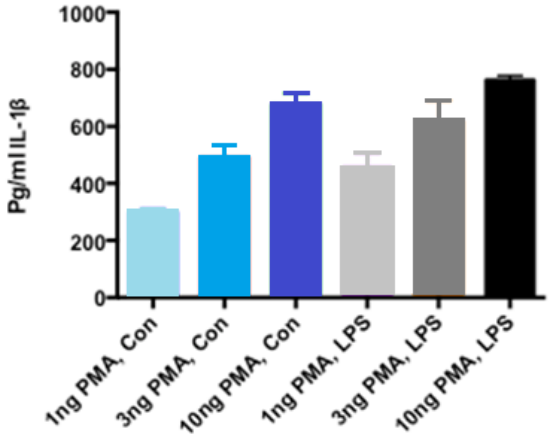

(Fig 4.17) IL-1β assay on 3 days PMA Differentiated U937 (Colony B)

P values indicate that all control group readings are significant; along with readings for the LPS-treated groups. However; a comparison cannot be made between the two groups; attributing to insignificant p values. The relationship demonstrated with colonies A and C is also apparent here- that PMA has a dose-related effect on the levels of TNFα generated in the U937 cells.

Control	LPS	Con x LPS
1ng x 3ng = yes; 0.0001	1ng x 3ng = yes; 0.0116	1ng x 1ng = yes; 0.0013
1ng x 10ng= yes; 0.0001	1ng x 10ng= yes; 0.0001	3ng x 3ng= ns
3ng x 10ng= yes; 0.0005	3ng x 10ng=yes; 0.0084	10ng x 10ng= yes; 0.0071

IL-1β; 18 hour differentiation; no treatment with MSU

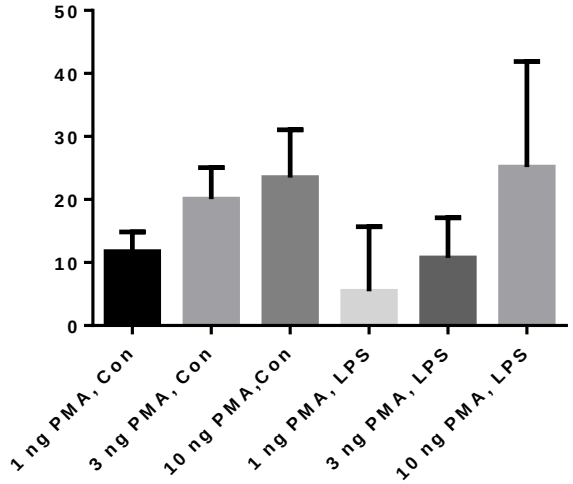

(Fig 4.19) IL-1β assay on 3 days PMA Differentiated U937 (Colony B)

Results from the graph proved to be insignificant (owing to their relative p values).

IL-1β; 18 hour differentiation with 4 hour treatment with MSU

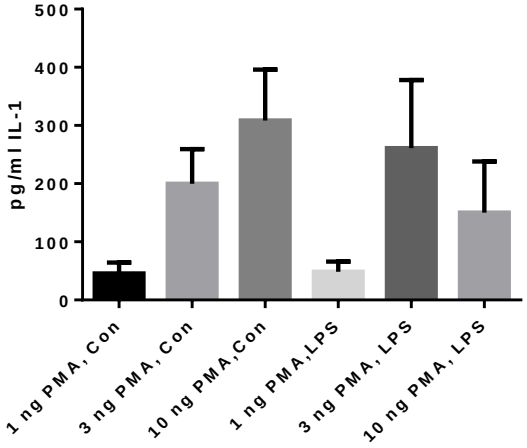

(Fig 4.20) IL-1β assay on 3 days PMA Differentiated U937 (Colony B)(MSU)

From the graph we can see an increase in IL-1β production when the concentration of PMA increases to 3ng. Unfortunately; further analysis is not possible due to the rest of the results being insignificant.

Control	LPS	Con x LPS
1ng x 3ng = yes; 0.0027	1ng x 3ng = ns	1ng x 1ng = ns
1ng x 10ng= yes; 0.0011	1ng x 10ng= ns	3ng x 3ng= ns
3ng x 10ng=ns	3ng x 10ng= ns	10ng x 10ng= ns

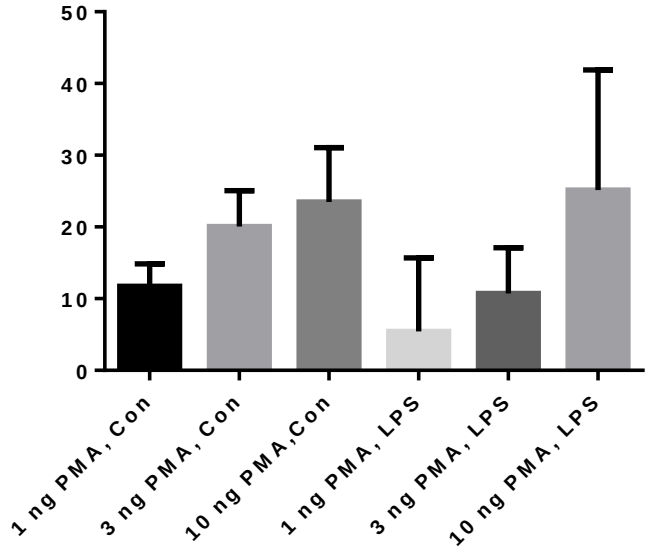

(Fig 4.21) IL-1β assay on 3 days PMA Differentiated U937 (Colony B)(MSU)

The two-way ANOVA concludes that the findings of this experiment are not statistically significant.

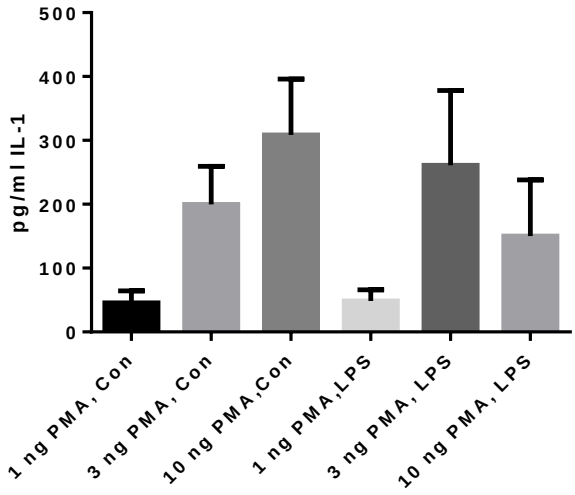

(Fig 4.22) IL-1β assay on 3 days PMA Differentiated U937 (Colony B)(MSU)

The column and row factors were found to be significant; along with the IL-1β readings attained by the 1ng and 3ng PMA control groups. There is a significant increase in IL-1β production in the controls when the concentration of PMA increases from 1ng to 3ng. The relative amount of IL-1β produced is larger in the group treated with MSU in comparison to the MSU-untreated group.

Control	LPS	Con x LPS
1ng x 3ng = yes; 0.0027	1ng x 3ng = ns	1ng x 1ng = ns
1ng x 10ng= yes; 0.0011	1ng x 10ng= ns	3ng x 3ng= ns
3ng x 10ng= ns	3ng x 10ng= ns	10ng x 10ng= ns

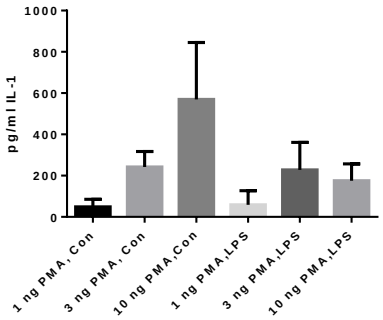

(Fig 4.23) IL-1β assay on 3 days PMA Differentiated U937 (Colony B)(MSU)

The column factor plus the 1ng and 3ng PMA control group measurements have been calculated to be statistically significant. As demonstrated in the previous graph; a significant increase in IL-1β production is evident when the concentration of PMA increases from 1ng to 3ng. In addition; IL-1β production appears to be higher in the groups treated with MSU than those groups left untreated.

Control	LPS	Con x LPS
1ng x 3ng = yes; 0.0036	1ng x 3ng = ns	1ng x 1ng = ns
1ng x 10ng= yes; 0.0097	1ng x 10ng= ns	3ng x 3ng= ns
3ng x 10ng= ns	3ng x 10ng= ns	10ng x 10ng= ns

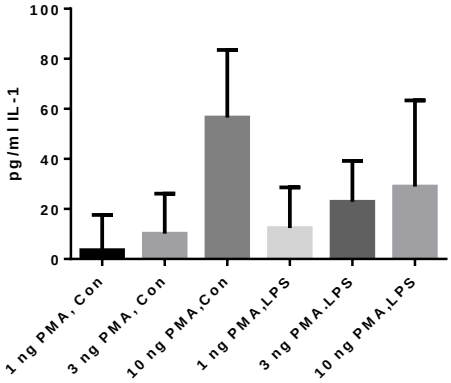

(Fig 4.24) IL-1β assay on 3 days PMA Differentiated U937 (Colony B)(MSU)

The two-way ANOVA shows that results are not statistically significant.4.5 Colony C; TNFα and IL-1β analysis

TNFα; 24 hour differentiation

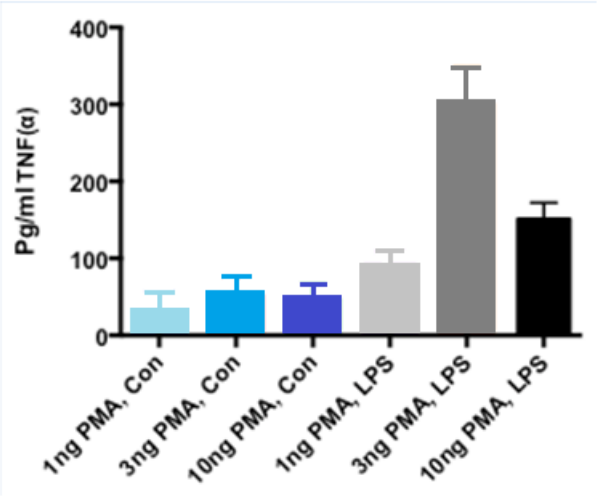

(1; 3;10ng/ml); washed and treated for 4 hours with medium (Con) or LPS (100U/(Fig 5.10) TNFα assay on 1 day PMA Differentiated U937 (Colony C). U937 cells were differentiated for 24 hours with indicated concentrations of PMA ml).

As shown with colony A and B; the greatest level of TNFα produced following LPS-activation is by the cells treated with 3ng PMA. Significant; albeit smaller readings were obtained at the 1ng and 10ng PMA concentrations; with the largest LPS-induced TNFα level at the 10ng concentration. The control readings were not significant and not used in the analysis.

Control	LPS	Con x LPS
1ng x 3ng = ns	1ng x 3ng = yes; 0.0004	1ng x 1ng = yes; 0.0100
1ng x 10ng= ns	1ng x 10ng= yes; 0.0107	3ng x 3ng= yes; 0.0012
3ng x 10ng= ns	3ng x 10ng= yes; 0.0074	10ng x 10ng= yes; 0.0033

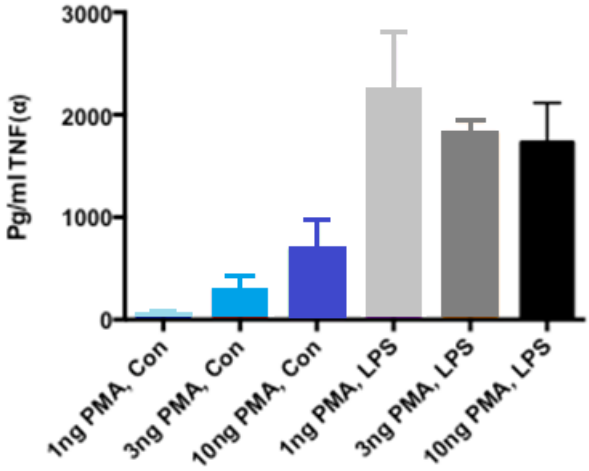

(Fig 5.11) TNFα assay on 3 days PMA Differentiated U937 (Colony C)

The readings for the 1ng and 3ng PMA controls were significant; with the highest TNFα production seen at the 3ng concentration. The readings for the LPS-treated cells are all statistically significant relative to the controls. TNFα levels were higher in the LPS-treated groups than the corresponding control group. In contrast to other figures; there is a dose-related reduction in TNFα production as the concentration of PMA increases.

Control	LPS	Con x LPS
1ng x 3ng = yes; 0.0134	1ng x 3ng = ns	1ng x 1ng = yes; 0.0005
1ng x 10ng= yes; 0.0072	1ng x 10ng= ns	3ng x 3ng= yes; 0.0001
3ng x 10ng= ns	3ng x 10ng= ns	10ng x 10ng= yes; 0.0209

TNFα; 72 hour differentiation

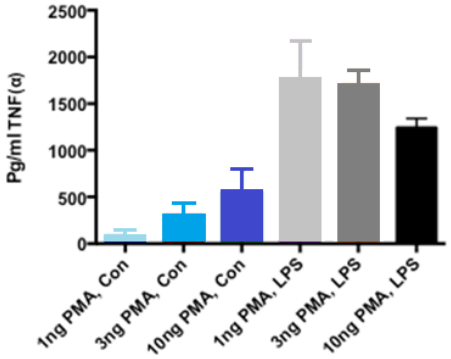

(Fig 5.12) TNFα assay on 3 days PMA Differentiated U937 (Colony C)

There is an apparent drop in TNFα production following LPS activation as the concentration of PMA rises. Comparing the levels produced by the 3ng PMA group treated with LPS and the control we can see that LPS stimulation induces higher TNFα levels than the controls. Compared to the 24 hour differentiation of the U937 cells; higher levels of TNFα were generated when left to differentiate for 72 hours.

Control	LPS	Con x LPS
1ng x 3ng = ns	1ng x 3ng = ns	1ng x 1ng = yes; 0.0002
1ng x 10ng= yes; 0.0123	1ng x 10ng= ns	3ng x 3ng= yes; 0.0003
3ng x 10ng= ns	3ng x 10ng= yes; 0.0134	10ng x 10ng= yes; 0.0105

IL-1β; 24 hours differentiation

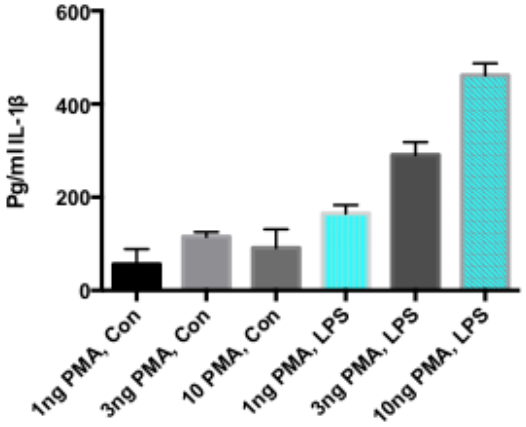

(Fig 5.13) IL-1β assay on 1 day PMA Differentiated U937 (Colony C)

The LPS-treated groups all provided significant results and from the graph we can see that as the PMA concentration increases the corresponding level of IL-1β also increases. The cells treated with 1ng PMA and LPS generated higher levels of IL-1β than the corresponding 1ng PMA control group.

Control	LPS	Con x LPS
1ng x 3ng = yes; 0.0127	1ng x 3ng = yes; 0.0003	1ng x 1ng = yes; 0.0011
1ng x 10ng= ns	1ng x 10ng= yes; 0.0001	3ng x 3ng= yes; 0.0001
3ng x 10ng= ns	3ng x 10ng= yes; 0.0001	10ng x 10ng= yes; 0.0001

IL-1β; 72 hour differentiation

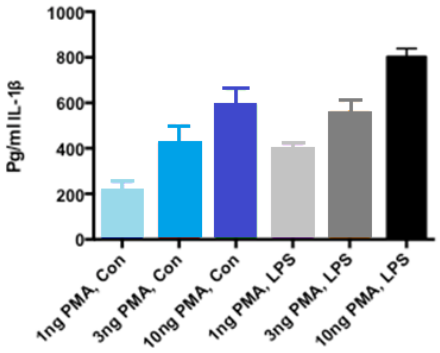

(Fig 5.15) IL-1β assay on 3 days PMA Differentiated U937 (Colony C)

All the readings are considered to be significant with reference to their corresponding p-values. At each concentration of PMA; we can see that a significantly higher level of IL-1β is generated by the LPS-treated groups compared to the controls. Compared to the 24 hour differentiation of the U937 cells; higher levels of IL-1β were generated when left to differentiate for 72 hours.

Control	LPS	Con x LPS
1ng x 3ng = yes; 0.0027	1ng x 3ng = yes; 0.0023	1ng x 1ng = yes; 0.0004
1ng x 10ng= yes; 0.0001	1ng x 10ng= yes; 0.0001	3ng x 3ng= yes; 0.0313
3ng x 10ng= yes; 0.0184	3ng x 10ng= yes; 0.0004	10ng x 10ng= yes; 0.0021

IL-β; 18 hours differentiation; no treatment with MSU

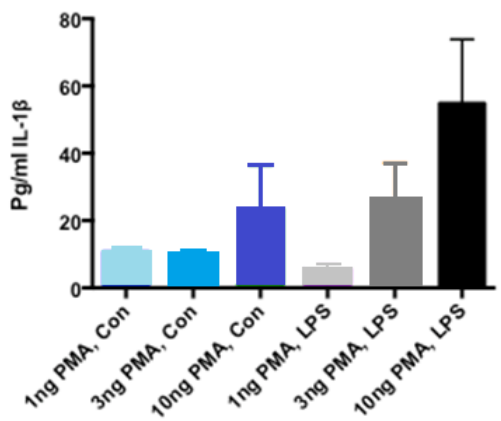

(Fig 5.17) IL-1β assay on 3 days PMA Differentiated U937 (Colony C)

P values indicate that the results obtained were not statistically significant and can therefore not be analysed.

Control	LPS	Con x LPS
1ng x 3ng = ns	1ng x 3ng = ns	1ng x 1ng = yes; 0.0095
1ng x 10ng= ns	1ng x 10ng= yes; 0.0112	3ng x 3ng= ns
3ng x 10ng= ns	3ng x 10ng= ns	10ng x 10ng= ns

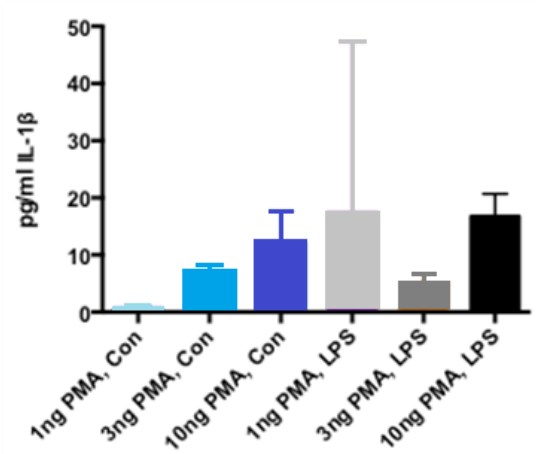

(Fig 5.18) IL-1β assay on 3 days PMA Differentiated U937 (Colony C)

The only significant readings that can be analyzed are those obtained for the 1ng and 3ng PMA control groups. We can see that higher IL-1β levels are generated at the 3ng concentration compared to the 1ng concentration.

Control	LPS	Con x LPS
1ng x 3ng = yes; 0.0001	1ng x 3ng = ns	1ng x 1ng = ns
1ng x 10ng= yes; 0.0066	1ng x 10ng= ns	3ng x 3ng= ns
3ng x 10ng= ns	3ng x 10ng= yes; 0.0015	10ng x 10ng= ns

IL-β; 18 hour differentiation and 4 hours treatment with MSU

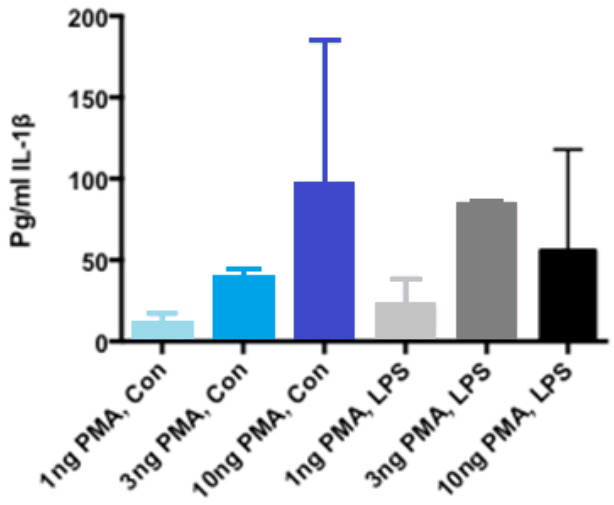

(Fig 5.19) IL-1β assay on 3 days PMA Differentiated U937 (Colony C)(MSU)

Interpretation of these results and comparison with the MSU-untreated group is difficult due to statistically insignificant results being obtained.

Control	LPS	Con x LPS
1ng x 3ng = yes; 0.0064	1ng x 3ng = yes; 0.0029	1ng x 1ng =ns
1ng x 10ng= ns	1ng x 10ng= ns	3ng x 3ng= yes; 0.0002
3ng x 10ng= ns	3ng x 10ng= ns	10ng x 10ng= ns

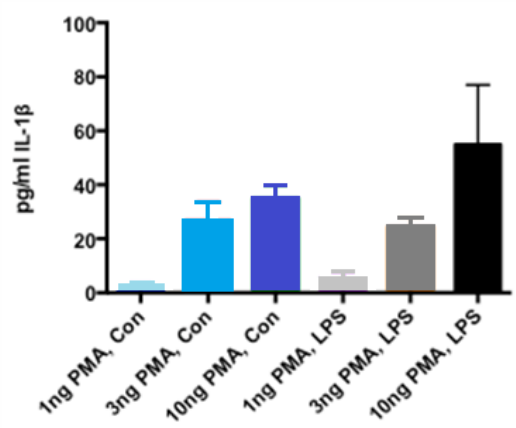

(Fig 5.20) IL-1β assay on 3 days PMA Differentiated U937 (Colony C)(MSU)

Comparing the 1ng and 3ng PMA control groups (treated with MSU); we can see a sharp rise in IL-1β production when the concentration of PMA rises to 3ng. This also occurs with the 1ng and 3ng PMA LPS-treated cells.

Control	LPS	Con x LPS
1ng x 3ng = yes; 0.0005	1ng x 3ng = yes; 0.0001	1ng x 1ng = ns
1ng x 10ng= yes; 0.0001	1ng x 10ng= yes; 0.0043	3ng x 3ng= ns
3ng x 10ng= ns	3ng x 10ng= ns	10ng x 10ng= ns

Chapter 5

5.0 Discussion

5.1 MTT

The MTT test is an indicator of cell viability *in vitro*; the more living cells available; the more enzymatic reactions and the more intense the colour result will be (with a corresponding increase in the spectrophotometric absorbance). Kim and Ha (2009) showed that LPS induces macrophage killing through the production of nitric oxide and the subsequent formation of the cytotoxic superoxide anions. Therefore; following LPS treatment we would expect the MTT level to drop due to the loss of cell viability.

A steady decline in the AU values can be seen in the graphs of all the colonies in response to an increasing PMA concentration. This may signify that PMA reduces cell viability and becomes toxic to the cells when it is present in too high a concentration. This trend is also witnessed in cells that underwent a 24 hour and 72 hour differentiation.

With regards to colony C; the 72 hour differentiation and 24 hour LPS-treatment group exhibited a contrasting result. As the PMA concentration increases; the AU values and cell viability increases. This contrasts with the findings of colonies A and B. However; the AU values were higher in the control group compared to the LPS-treated group; confirming that LPS treatment causes a reduction in cell viability.

The mean AU values in colony A's LPS-activated groups were generally higher than the control group. This insinuates that there was higher cell viability in the U937 cells stimulated with LPS; contrasting with Kim and Ha's findings (2009).

The results of colonies B and C replicate Kim and Ha's finding that LPS induces macrophage killing thus

reducing their viability. PMA can elicit a toxic effect on the cells when used in too high a concentration; as demonstrated with colonies A and B. However; due to the large number of insignificant results it would be worthwhile to repeat the experiments to determine the effect that treatment time of PMA and LPS have on the cells and the resultant AU levels.

5.2 TNFα

TNFα is produced by activated macrophages and is a key player in the recruitment of immune cells in order to compound an immune response to an invading pathogen. It also kicks starts phagocytosis and the production of cytokine IL-1.
A dose-related increase in TNFα production was seen in accordance with the PMA concentration. It is possible that the presence of dead cells induce an inflammatory reaction in the remaining living macrophages. As the concentration of PMA increases; the number of dead cells increases thus a larger inflammatory result is seen. Higher TNFα levels were generated by the LPS-treated groups in comparison with the controls; confirming the inflammatory response elicited by LPS. Compared the 24 hour and 72 hour differentiations; the longer the cells were exposed to PMA; the more extreme the inflammatory response seen. This suggests that PMA has a toxic effect on the U937 cells; if used for too long a time or at too high a concentration.
In colony B; higher levels of TNFα were generated by the control group than the group treated with LPS. This does not correspond to previous findings or the theory that LPS induces macrophage killing; and may be due to possible contaminants in the cell media.
A number of statistically insignificant results were generated in the TNFα analysis; leading to conflicting results. This highlights the importance of maintaining environmental parameters to generate reproducible results. A trend did happen to emerge from all the experiments- LPS-treatment led to a drop in viable macrophage numbers and a rise in TNFα release; due to the inflammatory response generated by the dead cells. This mirrors the findings from the MTT assay analysis and the work of Kim and Ha (2009)

5.3 IL-1β

Interleukin-1β (IL-1β); produced by activated macrophages; sets off an intracellular signalling cascade that subsequently causes the activation of transcription factors and expression of ROS-producing target genes. In monocytes; IL-1β interacts with NADPH oxidase in order to generate a pool of ROS (Bonizzi *et al.*; 1999).
Graphs for each colony indicate that high concentrations of PMA induce high levels of IL-1β; confirming the previous idea that PMA exhibits a dose-related toxicity towards macrophages; and as the death toll rises the ensuing inflammation becomes larger. Elevated levels of IL-1β are generated in the LPS-treated groups in comparison to the controls; reaffirming LPS's ability to induce cell death in macrophages (Kim and Ha; 2009)
The levels of IL-1β were more pronounced in cells left to differentiate for 72 hours compared to a 24 hour differentiation. This replicates previous findings that the toxicity demonstrated by PMA is both time and dose-related.
We would expect to see significant levels of IL-1β following MSU treatment due to its cytokine-inducing properties (Shi et al.; 2010). This effect can be witnessed in colony B; treatment with MSU induced higher levels of IL-1β than the untreated groups; confirming its action as a cytokine producer. Although results from the LPS and MSU treatment groups proved to be statistically insignificant; I would postulate that levels of IL-1β would be more pronounced following LPS stimulation and more so in higher concentrations of PMA.

5.4 RNAi

The gp91^{phox} protein is one of the primary elements of the NADPH-oxidase system in phagocytes (Segal *et al.*; 2012). A deficiency in the gp91^{phox} subunit has been associated with the development of CGD (e.g. Bjorgvinsdottir *et al.*; 1996; Rajakariar *et al.*; 2009; Sadat *et al.*; 2003; Zhen *et al.*;1993). It has been demonstrated in patients with a gp91^{phox} deficiency that a defective NADPH is at play; resulting in a lower production of ROS (Hill *et al.*; 2010). It is predicted that mutations in *CYBB*; encoding gp91^{phox} will lead to an insubstantial production of ROS via NADPH-oxidase; based upon findings of previous studies (for example; Bjorgvinsdottir *et al.*; 1996).
In studies with p47^{phox} mutant strains; high concentrations of macrophages were found to be became activated; thus producing more ROS through a NADPH oxidase-independent mechanism; leading to an augmented production of cytokines (Yi *et al*; 2010).
The p47^{phox} subunit of macrophages is comprised of a phox homology domain; a tandem SH3 domain; a polybasic region/auto-inhibitory region (PBR/AIR) and a proline-rich region. When the macrophages are in a resting state; the p47^{phox} subunit exists in an auto-inhibited form due to association of its tandem SH3 domain with PBR/AIR. When the macrophage becomes activated; PBR/AIR becomes phosphorylated and no longer exerts its inhibitory effects on the tandem SH3 domain of the p47^{phox} subunit; allowing it to carry out its function. The p47^{phox} subunit then travels to the plasma membrane to assemble with the other subunits of NADPH to generate the active form of NADPH (Yuzawa *et al.*; 2004). A mutation or knock out of the PBR subunit would mean the p47^{phox} subunit would not

exist in its naturally auto-inhibitory state and would therefore have travelled to the plasma membrane awaiting association with the other subunits.

The P47^{phox}siRNA-treated cells brought about the largest release of TNFα relative to the control; followed by gp91^{phox}siRNA and PBRsiRNA-treated cells. This suggests that knockout or mutation of the p47 subunit in macrophages leads to heightened TNFα release and inflammatory response; in comparison to the control. This reiterates the findings of Yi et al. (2012) who found that p47^{phox} mutant strains initiated a large inflammatory response and therefore higher TNFα release. The effects of a knocked out or mutated p47^{phox} subunit on IL-1β release compared to the control cannot be determined due to lack of significant results. The PBRsiRNA-treated cells spawned the smallest release of TNFα compared to the other siRNA-treated cells; however levels were greater than that of the control. In the absence of PBR; the p47 subunit may exist in a primed; activated form at the cell membrane. This may lead to the assembly of a sub-par NADPH which may not be able to generate as large an inflammatory response. However; more work needs to be carried out to better determine the exact mechanism behind this finding.

Hill et al (2010) found that gp91^{phox}-deficient patients had an attenuated NADPH function resulting in a smaller release of ROS and a less impressive immune reaction. This highlights the importance of this subunit in cultivating an immune response. Cells treated with gp91^{phox}siRNA produced less TNFα than the cells treated with p47^{phox}siRNA; confirming Hill's findings (2010) that there is a reduced immune response when gp91^{phox} is knocked out or present in a mutant form. It did; however; produce higher levels than the control which does not support the findings of Hill and colleagues (2010). Additionally; knock out of the gp91 subunit in the gp91^{phox}siRNA-treated cells resulted in a substantial increase in IL-1β release when compared to both the p47^{phox}siRNA-treated cells and the control which fails to correlate these findings as well.

The effect of MSU on IL-1β production in the siRNA-treated cells is not able to be deduced due to the statistically insignificant results being obtained.

6.0 Conclusion

When macrophages undergo stimulation through interactions with LPS; a component of gram-negative bacteria; macrophage cytotoxicity is usually the end result. This causes a subsequent drop in viable macrophage numbers and an ensuing inflammatory response towards the dead cells; as seen by the increase in TNFα and IL-1β release. PMA; which instigates the differentiation of U937 cells to macrophages; also demonstrates a cytotoxic effect upon the cells in a time and dose-dependent manner. Treatment with MSU resulted in an overall increase in IL-1β levels; attributable to its cytokine-inducing property. Unfortunately; statistical analysis revealed that a large proportion of the experimental readings were not credible; making it necessary to repeat the experiments. This will allow us to better determine the effect that relative treatment time of PMA and LPS has on the cells; and justify the results we have seen in these experiments. These results supported our hypothesis that mutations in various subunits of NADPH oxidase cause an altered macrophage response to infection. A knockout or mutation of the p47 subunit in macrophages was shown to result in an amplified release of TNFα in response to LPS treatment when compared to control. This may suggest that it has a redundant role in the inflammatory response; however; additional research in p47^{phox} mutant strains under a range of different experiment conditions will help to explain our findings. In the absence of the p47^{phox} auto-inhibitory component (PBR); the macrophages produced only a modest amount of TNFα. This may infer that in a non-inhibited state; the p47 subunit may behave differently upon macrophage stimulation; leading to an abnormal form of NADPH being activated. This is difficult to postulate in the absence of other statistically significant results; and further research on this topic is recommended. Mutating or knocking out other components of the p47 subunit; for example; its tandem SH3 domain; may enable us to resolve our observed findings.

Conflicting results were produced with reference to the inflammation generated by the mutant g91phox strains; prompting further analysis of this mutant and more diligence when performing the experiments.

CGD is a genetic disorder caused by a dysfunctional NADPH oxidase; unable to surmount a sufficient immune response to invading pathogens. Our findings reveal that mutations in various subunits of NADPH lead to a spectrum of different inflammatory responses being produced by macrophages. The results of this study can be applied to better our understanding of the pathogenesis of CGD and aid in the development of more targeted and effective therapies against CGD.

7.0 Statement of Author'sContribution

I did all the experiment under Dr Dean supervision except when using PMA in the differentiation, which Dr Dean did. My supervisor, Dr Dean Willis, conducted sections of the above methodology. Specific protocols include: stimulating the U937 with PMA, MTT assay, *preparing* the carbon monoxide and ruthenium drugs with DMSO, the preparation of the MSUs, IL-1β and the TNFα ELISA.

8.0 Acknowledgement

I would like to thank Dr Dean Willis for helpful discussions and advice, for training me in his lab and

helping me to use associated software, and for providing me with the human cells to study. My supervisor Dr Dean Willis has been an immense help and best tour guide through this journey. My utmost thanks and sincerity goes to him.

8.0 References

[1]. Asehnoune, K.; Strassheim, D.; Mitra, S.; Yeol Kim, J. And Abraham, E. (2004) Involvement of Reactive Oxygen Species in Toll-Like Receptor 4-Dependent Activation of NFκB. J Immunol; 172(4): 2522-29

[2]. Assari; T. (2006) Chronic Granulomatous Disease; fundamental stages in our understanding of CGD. Med Immunol; 5(4): 1-8.

[3]. Auron; P. E.; Webb; A. C.; Rosenwasser; L. J.; Mucci; S. F.; Rich; A.; Wolff; S. M. & Dinarello; C. A. (2007) Nucleotide sequence of human monocyte interleukin 1 precursor cDNA. Proc. Natl. Acad. Sci. USA 1984. 81: 7907-7911. J Immunol; 178(9): 5413-7.

[4]. Bianchi; M.; Hakkim; A.; Brinkmann; V.; Siler; U.; Seger; R. A.; Zychlinsky; A. & Reichenbach; J. (2009) Restoration of NET formation by gene therapy in CGD controls aspergillosis. Blood; 114(13): 2619-22.

[5]. Bjorgvinsdottir; H.; Zhen; L. & Dinauer; M. C. (1996) Cloning of murine gp91phox cDNA and functional expression in a human X-linked chronic granulomatous disease cell line. Blood; 87(5): 2005-10.

[6]. Bonizzi; G.; Piette; J.; Schoonbroodt; S.; Greimers; R.; Havard; L.; Merville; M. P. & Bours; V. (1999) Reactive oxygen intermediate-dependent NF-kappaB activation by interleukin-1beta requires 5-lipoxygenase or NADPH oxidase activity. Mol Cell Biol; 19(3): 1950-60.

[7]. Brinkmann; V.; Reichard; U.; Goosmann; C.; Fauler; B.; Uhlemann; Y.; Weiss; D. S.; Weinrauch; Y. & Zychlinsky; A. (2004) Neutrophil extracellular traps kill bacteria. Science; 303(5663): 1532-5.

[8]. Bu-Ghanim; H. N.; Segal; A. W.; Keep; N. H. & Casimir; C. M. (1995) Molecular analysis in three cases of X91- variant chronic granulomatous disease. Blood; 86(9): 3575-82.

[9]. Cartun; R. W. & Pedersen; C. A. (1989) An Immunocytochemical Technique Offering Increased Sensitivity and Lowered Cost with a Streptavidin-Horseradish Peroxidase Conjugate. Journal of Histotechnology; 12: 273-277.

[10]. Cross; A. R.; Yarchover; J. L. & Curnutte; J. T. (1994) The superoxide-generating system of human neutrophils possesses a novel diaphorase activity. Evidence for distinct regulation of electron flow within NADPH oxidase by p67-phox and p47-phox. J Biol Chem; 269(34): 21448-54.

[11]. Daigneault; M.; Preston; J. A.; Marriott; H. M.; Whyte; M. K. B. & Dockrell; D. H. (2010) The Identification of Markers of Macrophage Differentiation in PMA-Stimulated THP-1 Cells and Monocyte-Derived Macrophages. PLoS One; 5: e8668

[12]. De Ravin; S. S.; Naumann; N.; Cowen; E. W.; Friend; J.; Hilligoss; D.; Marquesen; M.; Balow; J. E.; Barron; K. S.; Turner; M. L.; Gallin; J. I. & Malech; H. L. (2008) Chronic granulomatous disease as a risk factor for autoimmune disease. J Allergy Clin Immunol; 122(6): 1097-103.

[13]. DeLeo; F. R.; Allen; L. A.; Apicella; M. & Nauseef; W. M. (1999) NADPH oxidase activation and assembly during phagocytosis. J Immunol; 163(12): 6732-40.

[14]. DeLeo; F. R.; Ulman; K. V.; Davis; A. R.; Jutila; K. L. & Quinn; M. T. (1996) Assembly of the human neutrophil NADPH oxidase involves binding of p67phox and flavocytochrome b to a common functional domain in p47phox. J Biol Chem; 271(29): 17013-20.

[15]. Gallin; J. I. & Buescher; E. S. (1983) Abnormal regulation of inflammatory skin responses in male patients with chronic granulomatous disease. Inflammation; 7(3): 227-32.

[16]. Galvez; J.; Saiz; E.; Linares; L. F.; Climent; A.; Marras; C.; Pina; M. F. & Castellon; P. (2002) Delayed examination of synovial fluid by ordinary and polarised light microscopy to detect and identify crystals. Ann Rheum Dis; 61: 444-7.

[17]. Gelman; A. (2005) Analysis of variance? Why it is more important than ever. The Annals of Statistics; 33: 1–53.

[18]. Grimm; M. J.; Vethanayagam; R. R.; Almyroudis; N. G.; Lewandowski; D.; Rall; N.; Blackwell; T. S. & Segal; B. H. (2011) Role of NADPH oxidase in host defense against aspergillosis. Med Mycol; 49 Suppl 1S144-9.

[19]. Gutierrez; M. J.; McSherry; G. D.; Ishmael; F. T.; Horwitz; A. A. & Nino; G. (2012) Residual NADPH oxidase activity and isolated lung involvement in x-linked chronic granulomatous disease. Case Rep Pediatr; 2012 974561.

[20]. Hazen; S. L.; Hsu; F. F.; Mueller; D. M.; Crowley; J. R. & Heinecke; J. W. (1996) Human neutrophils employ chlorine gas as an oxidant during phagocytosis. J Clin Invest; 98(6): 1283-9.

[21]. Heyworth; P. G.; Cross; A. R. & Curnutte; J. T. (2003) Chronic granulomatous disease. Curr Opin Immunol; 15(5): 578-84.

[22]. Hill; H. R.; Augustine; N. H.; Pryor; R. J.; Reed; G. H.; Bagnato; J. D.; Tebo; A. E.; Bender; J. M.; Pasi; B. M.; Chinen; J.; Hanson; I. C.; de Boer; M.; Roos; D. & Wittwer; C. T. (2010) Rapid genetic analysis of x-linked chronic granulomatous disease by high-resolution melting. J Mol Diagn; 12(3): 368-76.

[23]. Josephy; P. D.; Eling; T. & Mason; R. P. (1982) The horseradish peroxidase-catalyzed oxidation of 3;5;3';5'-tetramethylbenzidine. Free radical and charge-transfer complex intermediates. J Biol Chem; 257: 3669-75.

[24]. Kang; E. M.; Marciano; B. E.; DeRavin; S.; Zarember; K. A.; Holland; S. M. & Malech; H. L. (2011) Chronic granulomatous disease: overview and hematopoietic stem cell transplantation. J Allergy Clin Immunol; 127(6): 1319-34.

[25]. Khalilzadeh; S.; Bloorsaz; M. R.; Mansouri; D.; Baghaie; N.; Hakimi; S. & Velayati; A. A. (2006) Clinical and radiological aspects of chronic granulomatous disease in children: a case series from Iran. Iran J Allergy Asthma Immunol; 5(2): 85-8.

[26]. Kim; I. D. & Ha; B. J. (2009) Paeoniflorin protects RAW 264.7 macrophages from LPS-induced cytotoxicity and genotoxicity. Toxicol In Vitro; 23: 1014-9.

[27]. Krause; K. H. (2007) Aging: a revisited theory based on free radicals generated by NOX family NADPH oxidases. Exp Gerontol; 42(4): 256-62.

[28]. Kumar; D. 2008. Genetic and Genomic Approaches to Taxonomy of Human Disease. In: Kumar; D. & Weatherall; D. (eds.) Genomics and Clinical Medicine. Oxford: Oxford University Press.

[29]. Lehmann; M. H. (1998) Recombinant human granulocyte-macrophage colony-stimulating factor triggers interleukin-10 expression in the monocytic cell line U937. Mol Immunol; 35: 479-85

[30]. Lequin; R. M. (2005) Enzyme immunoassay (EIA)/enzyme-linked immunosorbent assay (ELISA). Clin Chem; 51: 2415-8.

[31]. Mamishi; S.; Zomorodian; K.; Saadat; F.; Gerami-Shoar; M.; Tarazooie; B. & Siadati; S. A. (2005) A case of invasive aspergillosis in CGD patient successfully treated with Amphotericin B and INF-gamma. Ann Clin Microbiol Antimicrob; 44.

[32]. Marciano; B. E.; Wesley; R.; De Carlo; E. S.; Anderson; V. L.; Barnhart; L. A.; Darnell; D.; Malech; H. L.; Gallin; J. I. & Holland; S. M. (2004) Long-term interferon-gamma therapy for patients with chronic granulomatous disease. Clin Infect Dis; 39(5): 692-9.

[33]. Martinon, G.; Mayor, A. And Tschopp, J. (2009) The Inflammasones: Guardians of the Body. Annu. Rev. Immunol; 27: 229-65

[34]. Mosser; D. M. & Edwards; J. P. (2008) Exploring the full spectrum of macrophage activation. Nat Rev Immunol; 8(12): 958-69.

[35]. OMIM Statistics. (2013) Online Mendelian Inheritance in Man Statistics for January 7; 2013 [Online]. John Hopkins University. Available: http://www.ncbi.nlm.nih.gov/Omim/mimstats.html [Accessed 04/07/13

[36]. Pao; M.; Wiggs; E. A.; Anastacio; M. M.; Hyun; J.; DeCarlo; E. S.; Miller; J. T.; Anderson; V. L.; Malech; H. L.; Gallin; J. I. & Holland; S. M. (2004) Cognitive function in patients with chronic granulomatous disease: a preliminary report. Psychosomatics; 45(3): 230-4.

[37]. Pizzolla; A.; Hultqvist; M.; Nilson; B.; Grimm; M. J.; Eneljung; T.; Jonsson; I. M.; Verdrengh; M.; Kelkka; T.; Gjertsson; I.; Segal; B. H. & Holmdahl; R. (2012) Reactive oxygen species produced by the NADPH oxidase 2 complex in monocytes protect mice from bacterial infections. J Immunol; 188(10): 5003-11.

[38]. Rajakariar; R.; Newson; J.; Jackson; E. K.; Sawmynaden; P.; Smith; A.; Rahman; F.; Yaqoob; M. M. & Gilroy; D. W. (2009) Nonresolving inflammation in gp91phox-/- mice; a model of human chronic granulomatous disease; has lower adenosine and cyclic adenosine 5'-monophosphate. J Immunol; 182(5): 3262-9.

[39]. Rapini, Ronald P.; Bolognia, Jean L.; Jorizzo, Joseph L. (2007) Dermatology;2(1)-4160-2999-0.

[40]. Roos; D.; Kuhns; D. B.; Maddalena; A.; Roesler; J.; Lopez; J. A.; Ariga; T.; Avcin; T.; de Boer; M.; Bustamante; J.; Condino-Neto; A.; Di Matteo; G.; He; J.; Hill; H. R.; Holland; S. M.; Kannengiesser; C.; Koker; M. Y.; Kondratenko; I.; van Leeuwen; K.; Malech; H. L.; Marodi; L.; Nunoi; H.; Stasia; M. J.; Ventura; A. M.; Witwer; C. T.; Wolach; B. & Gallin; J. I. (2010) Hematologically important mutations: X-linked chronic granulomatous disease (third update). Blood Cells Mol Dis; 45(3): 246-65.

[41]. Sadat; M. A.; Pech; N.; Saulnier; S.; Leroy; B. A.; Hossle; J. P.; Grez; M. & Dinauer; M. C. (2003) Long-term high-level reconstitution of NADPH oxidase activity in murine X-linked chronic granulomatous disease using a bicistronic vector expressing gp91phox and a Delta LNGFR cell surface marker. Hum Gene Ther; 14(7): 651-66.

[42]. Segal; A. W. & Abo; A. (1993) The biochemical basis of the NADPH oxidase of phagocytes. Trends Biochem Sci; 18(2): 43-7.

[43]. Segal; B. H.; Grimm; M. J.; Khan; A. N.; Han; W. & Blackwell; T. S. (2012) Regulation of innate immunity by NADPH oxidase. Free Radic Biol Med; 53(1): 72-80.

[44]. Segal; B. H.; Leto; T. L.; Gallin; J. I.; Malech; H. L. & Holland; S. M. (2000a) Genetic; biochemical; and clinical features of chronic granulomatous disease. Medicine (Baltimore); 79(3): 170-200.

[45]. Segal; B. H.; Sakamoto; N.; Patel; M.; Maemura; K.; Klein; A. S.; Holland; S. M. & Bulkley; G. B. (2000b) Xanthine oxidase contributes to host defense against Burkholderia cepacia in the p47(phox-/-) mouse model of chronic granulomatous disease. Infect Immun; 68(4): 2374-8.

[46]. Shi; Y.; Mucsi; A. D. & Ng; G. (2010) Monosodium urate crystals in inflammation and immunity. Immunol Rev; 233: 203-17.

[47]. Song; E.; Jaishankar; G. B.; Saleh; H.; Jithpratuck; W.; Sahni; R. & Krishnaswamy; G. (2011) Chronic granulomatous disease: a review of the infectious and inflammatory complications. Clin Mol Allergy; 9(1): 1-14.

[48]. Urban; C. F.; Reichard; U.; Brinkmann; V. & Zychlinsky; A. (2006) Neutrophil extracellular traps capture and kill Candida albicans yeast and hyphal forms. Cell Microbiol; 8(4): 668-76.

[49]. Uzel; G.; Orange; J. S.; Poliak; N.; Marciano; B. E.; Heller; T. & Holland; S. M. (2010) Complications of Tumor Necrosis Factor-± Blockade in Chronic Granulomatous Disease—Related Colitis. Clinical Infectious Diseases; 51(12): 1429-1434.

[50]. van de Veerdonk, F.L.; Smeekens, S.P.; Joosten, L.A.B.; Kullberg, B.J.; Dinarello, C.A.; van der Meer, J.W.M. and Netea, M.G. (2010) Reactive oxygen species-independent activation of the IL-1β inflammasome in cells from patients with chronic granulomatous disease. PNAS; 107(7): 3030-33

[51]. van den Berg; J. M.; van Koppen; E.; Ahlin; A.; Belohradsky; B. H.; Bernatowska; E.; Corbeel; L.; Espanol; T.; Fischer; A.; Kurenko-Deptuch; M.; Mouy; R.; Petropoulou; T.; Roesler; J.; Seger; R.; Stasia; M. J.; Valerius; N. H.; Weening; R. S.; Wolach; B.; Roos; D. & Kuijpers; T. W. (2009) Chronic granulomatous disease: the European experience. PLoS One; 4(4): e5234.

[52]. van Meerloo; J.; Kaspers; G. J. & Cloos; J. (2011) Cell sensitivity assays: the MTT assay. Methods Mol Biol; 731: 237-45.

[53]. Vignais; P. V. (2002) The superoxide-generating NADPH oxidase: structural aspects and activation mechanism. Cell Mol Life Sci; 59(9): 1428-59.

[54]. von Löhneysen; K.; Noack; D.; Wood; M. R.; Friedman; J. S. & Knaus; U. G. (2010) Structural insights into Nox4 and Nox2: motifs involved in function and cellular localization. Mol Cell Biol; 30(4): 961-75.

[55]. West; A. P.; Brodsky; I. E.; Rahner; C.; Woo; D. K.; Erdjument-Bromage; H.; Tempst; P.; Walsh; M. C.; Choi; Y.; Shadel; G. S. & Ghosh; S. (2011) TLR signalling augments macrophage bactericidal activity through mitochondrial ROS. Nature; 472(7344): 476-80.

[56]. Winkelstein; J. A.; Marino; M. C.; Johnston; R. B.; Jr.; Boyle; J.; Curnutte; J.; Gallin; J. I.; Malech; H. L.; Holland; S. M.; Ochs; H.; Quie; P.; Buckley; R. H.; Foster; C. B.; Chanock; S. J. & Dickler; H. (2000) Chronic granulomatous disease. Report on a national registry of 368 patients. Medicine (Baltimore); 79(3): 155-69.

[57]. Yi; L.; Liu; Q.; Orandle; M. S.; Sadiq-Ali; S.; Koontz; S. M.; Choi; U.; Torres-Velez; F. J. & Jackson; S. H. (2012) p47(phox) directs murine macrophage cell fate decisions. Am J Pathol; 180(3): 1049-58.

[58]. Yuzawa; S.; Ogura; K.; Horiuchi; M.; Suzuki; N.N.; Fujioka; Y.; Kataoka; M.; Sumimoto; H. And Inagaki; F. (2004) Solution Structure of the Tandem Src Homology 3 Domains of p47phox in an Autoinhibited Form. The Journal of Biological Chemistry; 279(28); 29752-29760.

[59]. Zhan; S.; Vazquez; N.; Wientjes; F. B.; Budarf; M. L.; Schrock; E.; Ried; T.; Green; E. D. & Chanock; S. J. (1996) Genomic structure; chromosomal localization; start of transcription; and tissue expression of the human p40-phox; a new component of the nicotinamide adenine dinucleotide phosphate-oxidase complex. Blood; 88(7): 2714-21.

[60]. Zhen; L.; King; A. A.; Xiao; Y.; Chanock; S. J.; Orkin; S. H. & Dinauer; M. C. (1993) Gene targeting of X chromosome-linked chronic granulomatous disease locus in a human myeloid leukemia cell line and rescue by expression of recombinant gp91phox. Proc Natl Acad Sci U S A; 90(21): 9832-6.

2/8/2023